

# Advanced safety filter based on SOS Control Barrier and Lyapunov Functions

Michael Schneeberger, Silvia Mastellone, Florian Dörfler

**Abstract**—This paper presents a novel safety filter framework that ensures both safety and the preservation of the legacy control action within a nominal region. This modular design allows the safety filter to be integrated into the control hierarchy without compromising the performance of the existing legacy controller within the nominal region. This is accomplished by formulating multiple Control Barrier Functions (CBFs) and Control Lyapunov-like Functions (CLFs) conditions, alongside a forward invariance condition for the legacy controller, as sum-of-squares constraints utilizing Putinar’s Positivstellensatz. Additionally, the state-dependent inequality constraints of the resulting Quadratic Program – encoding the CBF and CLF conditions – are designed to remain inactive within the nominal region, ensuring perfect tracking of the legacy control action. Our safety filter design is also the first to include quadratic input constraints, and does not need an explicit specification of the attractor, as it is implicitly defined by the legacy controller. To avoid the chattering effect and guarantee the uniqueness and Lipschitz continuity of solutions, the state-dependent inequality constraints of the Quadratic Program are selected to be sufficiently regular. Finally, we demonstrate the method in a detailed case study involving the control of a three-phase ac/dc power converter.

## I. INTRODUCTION

In various engineering applications, it is of much interest to endow a well-performant controller with safety guarantees by minimally changing its control action. This concept is commonly referred to as a *safety filter*, and a comprehensive overview of the subject can be found in [1]. An illustrative example is a finely-tuned control design based on linearization, which must be extended to adhere to hard state constraints in the nonlinear closed-loop system. We refer to such a well-performant controller as the *legacy controller*. A popular type of safety filters relies on solving a Quadratic Program (QP) at every state using a Control Barrier Function (CBF). By continuously solving the QP, the control action of the legacy controller is smoothly adjusted as the system approaches the boundary of the *safe set*  $\mathcal{X}_s$ . The main challenges in deploying such a safety filter lies in finding a viable CBF candidate and adhering to input constraints.

Even though safety filters based on a QP are well-established, they are frequently not adopted in current industrial setups due to their risk of altering the legacy control behavior during nominal operations. In practice, the legacy control parameters are often meticulously tuned and thoroughly

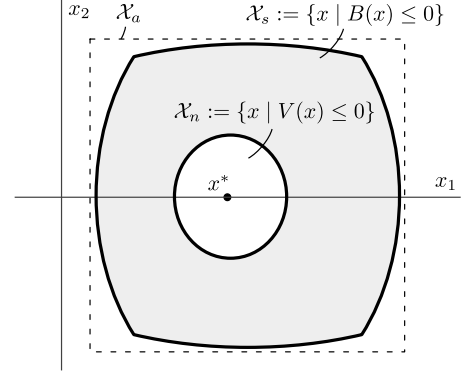


Fig. 1. The safe set  $\mathcal{X}_s$ , defined as the zero sublevel set of the CBF  $B(x)$ , specifies the set of states for which safety can be guaranteed. The safe set must be contained within the allowable set  $\mathcal{X}_a$ , which encodes the system’s state constraints. Finally, the nominal region  $\mathcal{X}_n$ , defined as the zero sublevel set of the CLF  $V(x)$ , must be contained within the safe set  $\mathcal{X}_s$ .

evaluated, typically involving extensive hardware-in-the-loop simulations, which require significant time and resources. As a result, the safety filter is expected to intervene only when the system approaches state constraints, meaning when it is leaving the nominal operating regime.

This paper presents a safety filter concept that guarantees the preservation of the legacy control action within a *nominal region*  $\mathcal{X}_n$ , which contains the desired closed-loop equilibrium point (or another attractor), as depicted in Figure 1. Unlike in a reach-avoid problem [2], the nominal region  $\mathcal{X}_n$  does not represent a predetermined set of target states. Instead, it is selected during the design process (often at an earlier stage) to encompass the nominal operating regime of the legacy controller while maintaining a sufficiently large transitional region for a smooth safety filter operation. The specifications are inherently more stringent than those of a standard safety filter, but may therefore be deployed in an industrial setup without interference in the original line-up.

Our safety filter is realized based on solving a Quadratic Constraint Quadratic Program (QCQP) at every state using multiple CBFs and Control Lyapunov-like Functions (CLFs). A QCQP instead of a simple QP is employed to encode quadratic input constraints, which are common, e.g., in power electronic applications. While CBF conditions (encoded as linear constraints of the QCQP) are used to ensure safety w.r.t.  $\mathcal{X}_s$ , we leverage the CLF condition (also encoded as linear constraints of the QCQP) to specify a dissipation rate ensuring a finite-time convergence from the boundary of the safe set to the nominal region  $\mathcal{X}_n$ . The finite-time convergence property

Michael Schneeberger and Silvia Mastellone are with the Institute of Electrical Engineering, FHNW, Windisch, Switzerland (e-mails: michael.schneeberger@fhnw.ch, silvia.mastellone@fhnw.ch), and Florian Dörfler is with the Department of Information Technology and Electrical Engineering, ETH Zürich, Switzerland, (e-mail: dorfler@control.ee.ethz.ch)

This work was supported by the Swiss National Science Foundation (SNSF) under NCCR Automation.

is not intended to enhance control performance but to ensure a rapid return to the nominal operating regime following an unforeseen event. We ensure that the nominal set contains the desired attractor by selecting it forward invariant with respect to the legacy controller. For identifying compatible CBF and CLF candidates that adhere to the linear and quadratic input constraints, as well as a solution for the QCQP at every state, we propose a Sum-of-Squares (SOS) optimization approach. Preserving the legacy control action is achieved by ensuring that the inequality constraints of the QCQP remain inactive within  $\mathcal{X}_n$ . This necessitates taking into account the legacy controller when searching for appropriate CBF and CLF candidates. To solve the resulting SOS program, we deploy an alternating algorithm that simultaneously searches for a feasible controller in the class of rational functions of the state.

The concept of our safety filter resembles the integration of a CLF with a CBF to attain both safety and stabilization. Such a unification, although just with a single function, has been initially proposed in [3]. The integration of both CLF and CBF into an optimization-based controller has since become a well-established concept, see the survey in [4]. Feasibility of such an optimization-based controller can be accomplished by introducing a slack variable that deactivates CLFs and CBFs based on their respective priorities, as shown in [5]. Alternatively, it is possible to compute compatible CLFs and CBFs using SOS tools, ensuring that for every state, there exists an input  $u$  satisfying all CBF and CLF conditions. In order to encode compatibility, there is one approach that introduces an SOS constraint for each CLF/CBF pair in the absence of inputs constraints [6]. The second approach establishes compatibility by introducing a polynomial or rational state-feedback controller, as outlined in [7], [8]. Such a controller can also be used to enforce linear input constraints, as demonstrated in [9]. Another noteworthy approach for imposing input constraints using a contrapositive statement, albeit without ensuring compatibility between CBFs and CLFs, is introduced in [10]. These approaches introduce auxiliary polynomials that render the resulting SOS problem bilinear in its decision variables. In [11], an alternating algorithm is proposed to solve this bilinear SOS problem. One challenge in seeking CLF and CBF candidates through an alternating algorithm is to identify an initial feasible point. In their work in [12], the authors constrained their search for an initial CBF to scalar functions of a specific form. This restriction allows to reformulate the problem with linearity in its decision variables.

After our previous work [8] on synthesizing a rational controller to find compatible CLF and multiple CBFs using SOS optimization, and through collaboration with industrial partners, we identified a recurring issue: any modifications to the existing legacy control architecture should not compromise the nominal control performance. A prime example for this is the integration of a safety filter. In this paper, we propose a novel way of implementing a safety filter without disturbing the legacy controller within the nominal region. The key advancements are summarized as follows:

- First, we propose a novel safety filter implementation that, by design, ensures finite-time convergence to the nominal region  $\mathcal{X}_n$  and perfect tracking of the legacy control action within that region.
- Second, multiple CBFs are used to increase flexibility of the resulting safe set. Instead of imposing each CBF condition separately, we relax these conditions when the corresponding CBF is not active, similar to the idea in [13]. Moreover, the CLF condition can also be relaxed by leveraging the forward invariance property of the CBFs, similar to [14] for autonomous systems.
- Third, the desired attractor (e.g., an equilibrium point or limit cycle), which is stabilized by the legacy controller in the nominal region, does not need to be specified explicitly, as it is implicitly specified through the legacy controller as a forward invariance condition.
- Fourth, we introduce a novel approach for encoding linear and quadratic input constraints on the rational controller. This ensures feasibility of the resulting QCQP-based controller, even in case of quadratic input constraints – an issue that, to the authors' knowledge, is unsolved.

To avoid chattering and guarantee the uniqueness and Lipschitz continuity of solutions, the state-dependent inequality constraints of the QCQP are selected to be sufficiently regular. Finally, we tested our framework on a detailed three-phase ac/dc converter system connected to an infinite bus, where we successfully synthesized a safety filter that ensures satisfaction of the state constraints given by the dc-link voltage and line current, while adhering to quadratic input constraints. We further tracked an a priori unspecified quadrature current reference of the ac/dc converter by integrating the reference as a state into a slightly modified system model.

The remainder of the paper is structured as follows: In Section II, the preliminaries and notation are discussed. Section III introduces the concept of the advanced safety filter, its properties, and the resulting problem statement. Numerical simulations, presented in Section VI, are provided to demonstrate the efficacy of our safety filter. Finally, Section VII concludes the paper.

## II. PRELIMINARIES & NOTATION

### A. Notation

The shorthand  $\mathcal{I}_t := \{1, 2, \dots, t\}$  designates a range of natural numbers from 1 to  $t$ .  $R[x]$  refers to the set of scalar polynomials in variables  $x \in \mathbb{R}^n$ , and  $\Sigma[x]$  refers to the set of scalar SOS polynomials in variables  $x \in \mathbb{R}^n$ . If  $p(x) \in \Sigma[x]$ , it can be expanded to

$$p(x) = Z(x)^T Q Z(x), \quad (1)$$

where  $Z(x)$  is a vector of monomials in  $x$ , and  $Q$  is a square positive semidefinite matrix.

Throughout the paper, we consider a polynomial control system, affine in the control action  $u \in \mathbb{R}^m$ , and described as

$$\dot{x} = F_c(x, u) = f(x) + G(x)u, \quad (2)$$

where  $x \in \mathbb{R}^n$  is the state,  $f(x) \in (R[x])^n$  is a polynomial vector field, and  $G(x) \in (R[x])^{n \times m}$  is a polynomial matrix. System (2) with a polynomial state feedback control policy  $u_{cl}(x) \in (R[x])^m$  results in a closed-loop system of the form

$$\dot{x} = F_{cl}(x) = f(x) + G(x)u_{cl}(x). \quad (3)$$

The interior of a set  $\mathcal{X} \subseteq \mathbb{R}^n$  is denoted by  $\text{int}(\mathcal{X})$ . A subset  $\mathcal{X} \subseteq \mathbb{R}^n$  is called *forward invariant* (cf. [15, Theorem 4.4]) with respect to system (3) if for every  $x(0) \in \mathcal{X}$ ,  $x(t) \in \mathcal{X}$  for all  $t \geq 0$ . A system (3) is called *safe* (cf. [16]) w.r.t. an *allowable set* of states  $\mathcal{X}_a \subseteq \mathbb{R}^n$  and the *safe set*  $\mathcal{X}_s \subseteq \mathbb{R}^n$ , if  $\mathcal{X}_s$  is forward invariant and  $\mathcal{X}_s \subseteq \mathcal{X}_a$ . We say that a controller  $u_{cl}(x)$  guarantees safety if the corresponding closed-loop system is safe.

*Assumption 1 (standing assumption):* In the following, the allowable set  $\mathcal{X}_a$  is assumed compact and regular.

### B. Putinar's Positivstellensatz

Before stating Putinar's P-satz, we need to introduce two preliminary definitions.

*Definition 1:* A quadratic module generated by polynomials  $f_2, \dots, f_n \in R[x]$  is defined by

$$\mathbf{M}(f_2, \dots, f_n) := \left\{ \gamma_0 + \sum_{i=2}^n \gamma_i f_i \mid \gamma_0, \dots, \gamma_n \in \Sigma[x] \right\}. \quad (4)$$

*Definition 2:* A quadratic module  $\mathbf{M}(f_2, \dots, f_n)$  is said to be *Archimedean* when there exists a polynomial  $f \in \mathbf{M}(f_2, \dots, f_n)$  such that  $\{x \in \mathbb{R}^n \mid f \geq 0\}$  is a compact set. The following theorem states Putinar's P-satz (cf. [17, Theorem 3.20]).

*Theorem 1:* Given polynomials  $f_1, \dots, f_n \in R[x]$  such that the quadratic module  $\mathbf{M}(f_2, \dots, f_n)$  is Archimedean, and

$$\{x \mid f_1(x) \leq 0, f_2(x) \geq 0, \dots, f_n(x) \geq 0\} = \emptyset, \quad (5)$$

then

$$f_1 \in \mathbf{M}(f_2, \dots, f_n). \quad (6)$$

In words, if the set in (5) is empty, Putinar's P-satz ensures that the polynomials  $\gamma_0, \gamma_2, \dots, \gamma_n$  defined in (4) exist, albeit without specifying their degree. To find these polynomials computationally requires to iteratively increase the degree of the polynomials until a solution can be found for (6). An increase in the degree of the polynomials will, however, deteriorate computation time. For many practical examples of interest, however, low-degree polynomials suffice.

Condition (6) can also be expressed more explicitly through the condition that there exists  $\gamma_1, \gamma_2, \dots, \gamma_n \in \Sigma[x]$  such that

$$\gamma_1 f_1 - \gamma_2 f_2 - \dots - \gamma_n f_n \in \Sigma[x]. \quad (7)$$

Assuming the empty-set condition in (5) holds, a solution to (7) involving  $\gamma_1(x) = 1$  is guaranteed by Putinar's P-satz to exist when the degrees of the polynomials are possibly unbounded. In this case, the introduction of the SOS polynomial  $\gamma_1(x)$  needlessly increases the set of feasible polynomials  $f_1(x)$ . However, when the degrees of the polynomials are truncated, this assertion may no longer hold true, justifying the utilization of  $\gamma_1(x)$ . For the rest of the paper, we refer to both inclusions, (6) and (7), as an *SOS constraint*.

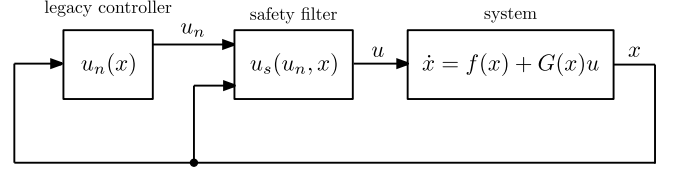


Fig. 2. The safety filter  $u_s(u_n, x)$  adjusts the legacy control action  $u_n(x)$  – if necessary – to guarantee safe operation.

## III. SPECIFICATIONS AND PROBLEM STATEMENT

### A. Specifications

The concept of a *safety filter* (see Figure 2) is based on the idea of enhancing the behavior of a previously designed *legacy controller*  $u_n(x)$  with safety guarantees. The safety filter adjusts the control action of the legacy controller, ideally in a minimal way, to render the system safe with respect to an allowable set  $\mathcal{X}_a$ , encoding the state constraints, and a safe set  $\mathcal{X}_s$ . The safe set denotes a set of states that is forward invariant for some state feedback controller. Therefore, we require that the safe set is strictly contained within the allowable set, i.e.,

$$\mathcal{X}_s \subseteq \mathcal{X}_a. \quad (8)$$

The safe set is preferably chosen large in volume to closely approximate the allowable set.

The standard characterization of a safety filter does not specify the extent to which it is allowed to alter the legacy control action. This can be problematic, as the safety filter might inadvertently undermine the desired behavior of the legacy controller. In contrast, our *advanced safety filter*  $u_s(x)$  specifies a distinct region  $\mathcal{X}_n$ , where the safety filter remains inactive, that is, for all  $x \in \mathcal{X}_n$ :

$$u_s(x) = u_n(x). \quad (9)$$

This *nominal region*  $\mathcal{X}_n$  is required to be forward invariant under the legacy control  $u_n(x)$ , and to be strictly contained within the safe set, i.e.,

$$\mathcal{X}_n \subsetneq \mathcal{X}_s. \quad (10)$$

For a legacy controller that stabilizes the closed-loop system to an attractor within  $\mathcal{X}_a$ , a forward invariant set does always exist.

Moreover, the advanced safety filter should preserve such a stability guarantee across the entire safe set. This is already accomplished within the nominal region  $\mathcal{X}_n$  due to its forward invariance property. Hence, we only need to additionally ensure a finite-time convergence to  $\mathcal{X}_n$  for all trajectories originating within the *transitional region*, defined as:

$$\mathcal{X}_t := \mathcal{X}_s \setminus \text{int}(\mathcal{X}_n), \quad (11)$$

where  $\text{int}(\mathcal{X}_n)$  denotes the interior of a set  $\mathcal{X}_n$ .

*Remark 1:* The volume of  $\mathcal{X}_t$  must be balanced with the volume of  $\mathcal{X}_n$ . A larger  $\mathcal{X}_t$  ensures a smooth behavior of the safety filter when returning the system to  $\mathcal{X}_n$ , while a larger  $\mathcal{X}_n$  provides a wider nominal region where the safety filter does not modify the legacy control action.

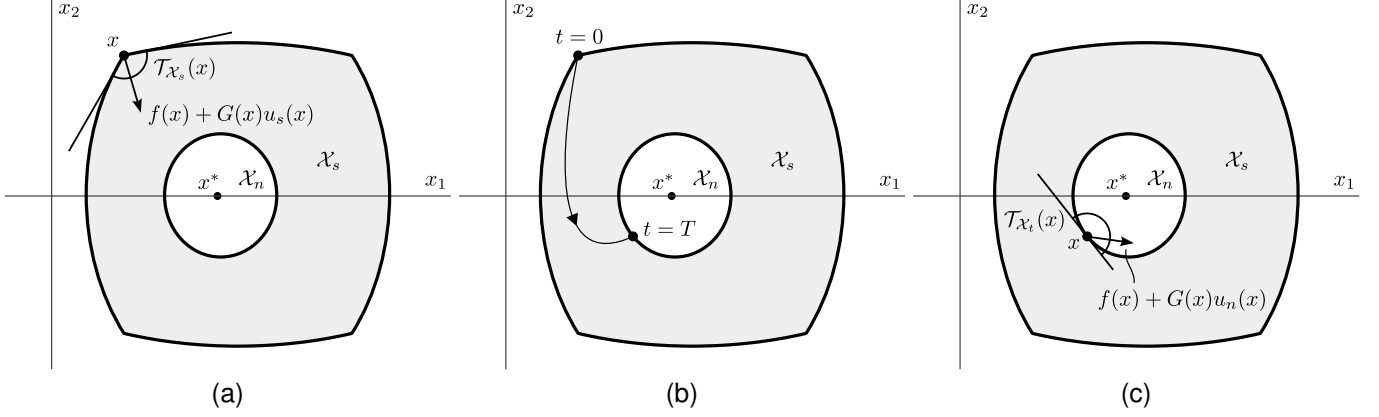


Fig. 3. The advanced safety filter is characterized by the following specifications: (a) the safe set  $\mathcal{X}_s$  is forward invariant as encoded in (15), (b) it ensures finite-time convergence towards the nominal region  $\mathcal{X}_n$  as encoded in (17), and (c) the nominal region is forward invariant under the legacy controller  $u_n(x)$  as encoded in (19) assuming  $d(x) = 0$ .

### B. CBF and CLF conditions formalizing the specifications

We employ control Lyapunov and barrier functions to encode the specification from the previous subsection by introducing energy-like scalar functions. In the process, we define the safe set as the intersection of zero-sublevel sets of multiple continuously differentiable functions to closely fit the algebraic structure of the allowable set

$$\mathcal{X}_a := \{x \mid w_i(x) \leq 0 \ \forall i \in \mathcal{I}_t\} = \bigcap_{i \in \mathcal{I}_t} \mathcal{X}_{a,i}, \quad (12)$$

where  $w_i \in R[x]$ ,  $i \in \mathcal{I}_t$ , are scalar polynomials, and their zero-sublevel sets  $\mathcal{X}_{a,i} := \{x \mid w_i(x) \leq 0\}$  are assumed to be compact. This compactness condition is important for applying Putinar's P-satz in the following section of the paper, and it is not restrictive for the applications we have in mind.

The forward invariance property of the safe set can be asserted by a scalar function  $B(x)$  defined as the point-wise maximum of a set of continuously differentiable functions  $B_i : \mathbb{R}^n \rightarrow \mathbb{R}$  indexed by  $\mathcal{I}_t$ :

$$B(x) := \max_{i \in \mathcal{I}_t} B_i(x), \quad (13)$$

such that the safe set is given by the intersection of the individual zero-sublevel sets:

$$\mathcal{X}_s := \{x \mid B(x) \leq 0\} = \bigcap_{i \in \mathcal{I}_t} \mathcal{X}_{s,i},$$

where  $\mathcal{X}_{s,i} := \{x \mid B_i(x) \leq 0\}$ . Taking the intersection of multiple functions  $B_i(x)$  allows for greater flexibility to increase the volume of the safe set compared to using the zero-sublevel set of a single CBF function. This is because the zero-sublevel sets of each  $B_i(x)$  can extend beyond the allowable set, provided their intersection remains within the allowable set. In contrast, the zero-sublevel set of a single CBF must be fully contained within the allowable set. Hence, we encode the containment condition in (8) as:

$$\mathcal{X}_{s,i} \subseteq \mathcal{X}_{a,i}, \quad (14)$$

for every  $i \in \mathcal{I}_t$ . This can be seen from  $\bigcap_{i \in \mathcal{I}_t} \mathcal{X}_{s,i} \subseteq \bigcap_{i \in \mathcal{I}_t} \mathcal{X}_{a,i}$  implying  $\mathcal{X}_s \subseteq \mathcal{X}_a$ . Here, we assume that the CBF

$B(x)$  is defined using the same number of polynomials  $B_i(x)$  as polynomials  $w_i(x)$  that define the allowable set. To reduce the number of decision variables in  $B(x)$ , we can equate certain polynomials  $B_i(x)$  in the resulting SOS problem. This reduction results in a safe set comprising fewer distinct subsets  $\mathcal{X}_{s,i}$  compared to the subsets  $\mathcal{X}_{a,i}$  that define the allowable set.

*Assumption 2:* We assume the safe set  $\mathcal{X}_s$  to be regular in the sense that  $\forall x \in \mathcal{X}_s, \exists z \in \mathbb{R}^n, \forall i \in \mathcal{I}_t$  [18, Definition 4.9]:

$$B_i(x) + \nabla B_i(x)^T z < 0$$

The regularity assumption in Assumption 2 is a mild one, and it generically holds true, if  $B_i(x)$  is chosen as a polynomial. It implies that the interior of the safe set is given by  $\text{int}(\mathcal{X}_s) = \{x \mid B_i(x) < 0 \ i \in \mathcal{I}_t\}$ . Examples of polynomials that violate the regularity assumption can be found in [18, Chapter 4.2].

To ensure forward invariance of  $\mathcal{X}_s$ , as shown in Figure 3(a),  $B(x)$  needs to satisfy Nagumo's theorem, that is,  $\forall x \in \partial \mathcal{X}_s, \exists u \in \mathbb{R}^m$  (cf. [18, Nagumo's Theorem 4.7]):

$$f(x) + G(x)u \in \mathcal{T}_{\mathcal{X}_s}(x), \quad (15)$$

where, under Assumption 2, the tangent cone is defined by

$$\mathcal{T}_{\mathcal{X}_s}(x) := \{z \mid \nabla B_i(x)^T z \leq 0 \ i \in \text{Act}(x)\}, \quad (16)$$

and  $\text{Act}(x) := \{i \in \mathcal{I}_t \mid B_i(x) = 0\}$  denotes the set of active constraints. The function  $B(x)$  in (13) satisfying (15) and (16) will henceforth be referred to as a *Control Barrier Function* (CBF).

Compared to the standard safety filter, our approach also require finite-time convergence towards  $\mathcal{X}_n$ , as outlined in the specifications. This is asserted by a Control Lyapunov Function (CLF) defined by a continuously differentiable function  $V : \mathbb{R}^n \rightarrow \mathbb{R}$ . This function needs to satisfy a Control Lyapunov-like condition in the transitional region  $\mathcal{X}_t$ , as shown in Figure 3(b). Namely,  $\forall x \in \mathcal{X}_t, \exists u \in \mathbb{R}^m$ :

$$\nabla V(x)^T (f(x) + G(x)u) + d(x) \leq 0 \quad (17)$$

with *dissipation rate*

$$d(x) := \lambda(x) (V(x) + V_0) > 0, \quad (18)$$

where  $\lambda : \mathbb{R}^n \rightarrow \mathbb{R}_{>0}$  is a Lipschitz continuous function, and  $V_0 \leq \min_x (V(x))$  is a constant value, ensuring  $d(x)$  is strictly positive (and thus  $V(x)$  strictly decaying) in the transitional region  $\mathcal{X}_t$ . By utilizing a strictly positive function  $d(x)$ , the CLF condition can be expressed as a non-strict inequality condition similar to the CBF condition – a crucial distinction for the subsequent arguments presented in the next section. We define the nominal region as the zero sublevel set of  $V(x)$ :

$$\mathcal{X}_n := \{x \mid V(x) \leq 0\}.$$

Consequently, the transitional region is given by:

$$\mathcal{X}_t := \{x \mid B(x) \leq 0 \leq V(x)\}.$$

The next lemma establishes the finite-time convergence property associated with the CLF  $V(x)$ . Its proof can be found in the appendix.

**Lemma 1:** Given a Lipschitz-continuous controller  $u_s : \mathbb{R}^n \rightarrow \mathbb{R}^m$  that satisfies condition (17) with  $u := u_s(x)$  and renders the safe set  $\mathcal{X}_s$  forward invariant, then for all trajectories of system (3) starting in the safe set  $\mathcal{X}_s$  there exists some finite  $T \geq 0$  such that  $x(t) \in \mathcal{X}_n$  for all  $t \geq T$ .

Additionally, to make the nominal region forward invariant w.r.t. the legacy controller  $u_n(x)$ , as depicted in Figure 3(c), we propose the condition that  $\forall x \in \partial\mathcal{X}_n$ :

$$\nabla V(x)^T (f(x) + G(x)u_n(x)) + d(x) \leq 0. \quad (19)$$

Notice that forward invariance also follows with  $d(x) = 0$ . By adopting a slightly stricter forward invariance condition in (19) involving the strictly positive dissipation rate  $d(x)$ , we ensure the existence of the safety filter implementation as specified in Section V.

**Remark 2:** As the volume of the transitional region  $\mathcal{X}_t$  approaches zero, the proposed safety filter transitions into a safety filter based on a single CBF  $V(x) = B_1(x) = \dots = B_t(x)$ , where the CBF and CLF condition (15) and (17) are automatically satisfied by the forward invariance condition (19) of the legacy controller. Therefore, feasible CBF and CLF candidates can be found (in the limit) if a forward invariant set for the system, governed by the legacy controller, exists and is fully contained within the allowable set.

### C. Problem statement

The challenge of deriving the advanced safety filter can be divided into two subproblems. The first subproblem resolves around finding  $B(x)$  and  $V(x)$  that fulfill the CBF and CLF condition outlined in the preceding section. This involves constructing a rational controller  $u_{\text{SOS}}(x)$  to prove the compatibility of the CLF and CBF conditions in (15) and (17). Furthermore, we necessitate the assurance of the forward invariance condition of the legacy controller as defined in (19).

**Problem 1:** Given a dynamical system (3), an allowable set of states  $\mathcal{X}_a$  and a legacy controller  $u_n(x) \in \mathcal{U}$ , find scalar functions  $B(x) : \mathbb{R}^n \rightarrow \mathbb{R}$  and  $V(x) : \mathbb{R}^n \rightarrow \mathbb{R}$  such that:

- (set containment) the containment conditions in (8) and (10) are satisfied,

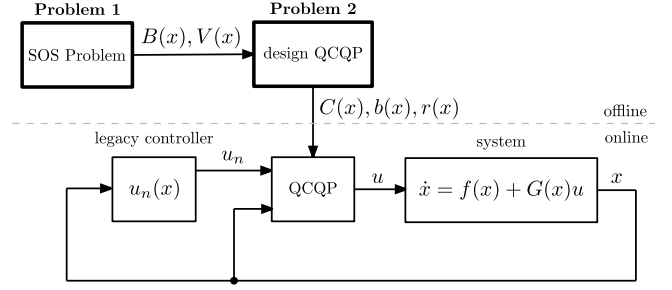


Fig. 4. Problem 1 involves searching for compatible CBF  $B(x)$  and CLF  $V(x)$  using SOS tools. Based on  $B(x)$  and  $V(x)$ , the linear constraints of the QCQP given by  $C(x)$ ,  $b(x)$  and  $r(x)$  are determined.

- (finite-time convergence) the CLF condition in (17) is satisfied,
- (forward-invariance of  $\mathcal{X}_s$ ) CBF and CLF conditions in (15) and (17) are satisfied on  $\partial\mathcal{X}_s$  for the same  $u$ ,
- (forward-invariance of  $\mathcal{X}_n$ ) legacy control condition in (19) is satisfied,
- (objective) CBF  $B(x)$  maximizes the volume of the safe set, denoted by  $\text{vol}(\mathcal{X}_s)$ .

For the second subproblem, a safety filter  $u_s(x)$  is constructed from  $B(x)$  and  $V(x)$ , which is guaranteed to be feasible and Lipschitz-continuous, entailing a smooth transitioning from the safety filter operation to the legacy control operation.

**Problem 2:** Given a dynamical system (3), a Lipschitz-continuous legacy controller  $u_n(x)$ , a CBF  $B(x)$  and CLF  $V(x)$ , as specified in Problem 1, find state-feedback control law  $u_s(x)$  that is feasible for all  $x \in \mathbb{R}^n$ , satisfies the CBF and CLF conditions (15) and (17) with  $u := u_s(x)$ , coincides with  $u_n(x)$  on  $\mathcal{X}_n$  (cf. (9)), and is Lipschitz-continuous.

In Section IV, we delve into a solution for Problem 1, while a solution for Problem 2 is derived in Section V.

## IV. CONSTRUCTING CBF AND CLF USING SOS OPTIMIZATION

### A. SOS formulation of CBF and CLF conditions

The objective of this subsection is to derive sufficient SOS conditions that encode the CBF condition on  $\mathcal{X}_s$  and  $\mathcal{X}_n$ , as specified in (15) and (19), and the CLF condition, as specified in (17). We further demonstrate that these SOS conditions are not overly conservative and pose no practical concerns.

The CBF condition in (15) involves the set of active constraints  $\text{Act}(x)$ , a construction that cannot be directly expressed as an SOS constraint. To address this issue, we first consider the polynomials  $B_i(x)$ ,  $i \in \mathcal{I}_t$ , defining the CBF  $B(x)$  in (13), as independent CBFs in their own right. By ensuring compatibility among these CBFs  $B_i(x)$  as proposed in [8], we demonstrate sufficiency of the resulting SOS constraints with respect to CBF condition in (15) (involving the desired CBF  $B(x)$ ). The CBF condition for each  $B_i(x)$ ,  $i \in \mathcal{I}_t$ , is expressed as  $\forall x \in \{x \in \mathcal{X}_s \mid B_i(x) = 0\}, \exists u \in \mathbb{R}^m$ :

$$\nabla B_i(x)^T (f(x) + G(x)u) \leq 0. \quad (20)$$

Another challenge in converting conditions (20) and (17) to SOS constraints is the presence of the existential quantifier

$\exists u \in \mathbb{R}^m$ . However, following the approach in [11], we can reformulate these conditions without the need for an existential quantifier. The CBF condition (20) can be expressed as  $\forall x \in \{x \in \mathcal{X}_s \mid B_i(x) = 0, \nabla B_i(x)^T G(x) = 0\}$ :

$$\nabla B_i(x)^T f(x) \leq 0. \quad (21)$$

Similarly, the CLF condition in (17) can be formulated as  $\forall x \in \{x \in \mathcal{X}_t \mid \nabla V(x)^T G(x) = 0\}$ :

$$\nabla V(x)^T f(x) + d(x) \leq 0. \quad (22)$$

In order to render the problem tractable, we restrict our attention to polynomial candidates  $B_i \in R[x]$ ,  $i \in \mathcal{I}_t$ , and polynomial candidate  $V \in R[x]$ . We then apply Putinar's P-satz, as stated in Theorem 1, on a slightly more stringent conditions compared to (19), (21) and (22), where the inequality is replaced by a strict inequality. These more stringent conditions are summarized as the following empty-set conditions,  $i \in \mathcal{I}_t$ :

$$\{x \mid -\nabla B_i(x)^T f(x) \leq 0, \nabla B_i(x)^T G(x) = 0, B_i(x) = 0, -B_{\mathcal{I}_t}(x) \geq 0\} = \emptyset \quad (23a)$$

$$\{x \mid -\nabla V(x)^T f(x) - d(x) \leq 0, \nabla V(x)^T G(x) = 0, V(x) \geq 0, -B_{\mathcal{I}_t}(x) \geq 0\} = \emptyset \quad (23b)$$

$$\{x \mid \nabla V(x)^T (f(x) + G(x)u_n(x)) + d(x) \leq 0, V(x) = 0\} = \emptyset, \quad (23c)$$

where  $B_{\mathcal{I}_t}(x) = [B_1(x) \ \dots \ B_t(x)]^T$  is a vector of CBFs. The resulting SOS constraints are summarized below. A detailed derivation of the SOS constraint (24) from the empty-set condition (23) is given in the supplementary material in [19].

$$-\nabla B_i^T (s_i f + G p_i) \in \mathbf{M}(B_i, -B_{\mathcal{I}_t}) \quad (24a)$$

$$-\nabla V^T (s_0 f + G p_0) - s_0 d \in \mathbf{M}(V, -B_{\mathcal{I}_t}) \quad (24b)$$

$$-\nabla V^T (f + G u_n) - d \in \mathbf{M}(V, -V), \quad (24c)$$

for some  $p_i \in (R[x])^m$  and  $s_i \in \Sigma[x]$ ,  $i \in \{0\} \cup \mathcal{I}_t$ . For clarity, we omit the brackets and variables in the function notation. To achieve the simultaneous satisfaction of CBF and CLF conditions (15) and (17) with a single input  $u := p(x)/s(x)$  on  $\partial \mathcal{X}_s$ , as specified in Problem 1, we equate the polynomials  $p_i(x)$  and  $s_i(x)$ ,  $i \in \{0\} \cup \mathcal{I}_t$ . The resulting SOS constraints are given as:

$$-\nabla B_i^T (s f + G p) \in \mathbf{M}(B_i, -B_{\mathcal{I}_t}) \quad (25a)$$

$$-\nabla V^T (s f + G p) - s d \in \mathbf{M}(V, -B_{\mathcal{I}_t}) \quad (25b)$$

$$-\nabla V^T (f + G u_n) - d \in \mathbf{M}(V, -V), \quad (25c)$$

for  $i \in \mathcal{I}_t$ , and some  $p \in (R[x])^m$ , and  $s \in \Sigma[x]$ .

*Remark 3:* The polynomials  $p(x)$  and  $s(x)$  induce (after dividing (25a) and (25b) by  $s(x)$ ) a rational controller  $u_{\text{SOS}}(x) := p(x)/s(x)$ , employed to prove compatibility of the CBFs  $B_i(x)$  and CLF  $V(x)$ .

The proof of Lemma 2 can be found in the appendix.

*Lemma 2:* If  $s(x) > 0$  and Assumption 2 is satisfied, then the SOS constraints in (25) are sufficient conditions for the CBF and CLF property in (15), (17) and (19) to hold simultaneously with  $u := p(x)/s(x)$ .

The SOS constraints in (25) imply the inequalities since  $p \in \Sigma[x]$  implies  $p(x) \geq 0$ :

$$\nabla B_i^T (s f + G p) + \gamma_{0,i} B_i - \gamma_{1,i}^T B_{\mathcal{I}_t} \leq 0 \quad (26a)$$

$$\nabla V^T (s f + G p) + s d + \gamma_{0,0} V - \gamma_{1,0}^T B_{\mathcal{I}_t} \leq 0 \quad (26b)$$

$$\nabla V^T (f + G u_n) + d + \gamma_n V \leq 0, \quad (26c)$$

for some  $\gamma_{0,i}, \gamma_n \in R[x]$ ,  $p \in (R[x])^m$ ,  $s, \gamma_{0,0} \in \Sigma[x]$ , and  $\gamma_{1,i}, \gamma_{1,0} \in (\Sigma[x])^t$ ,  $i \in \mathcal{I}_t$ .

Lemma 2 only provides sufficient conditions. However, adding an arbitrary small perturbation  $\epsilon > 0$  to the SOS constraints in (25) results in necessary conditions when restricting to rational controllers  $u_{\text{SOS}}(x) = p(x)/s(x)$ . This is because (15), (17) and (19) with  $u := u_{\text{SOS}}(x)$  imply strict inequalities involving  $\epsilon$  as follows:  $p(x) \leq 0$  implies  $p(x) - \epsilon < 0$ . These strict inequalities imply the SOS constraints (25) perturbed by  $\epsilon$  according to Theorem 1. Hence, for all practical purposes, the solution set of the SOS constraints in (25) encompasses the desired set of CBFs and CLFs.

### B. SOS formulation of input constraints

In the following, we consider two types of inputs constraints: linear and quadratic input constraints. Consider the linear input constraint set

$$\mathcal{U} = \{u \mid Au \leq b\}, \quad (27)$$

where  $A \in \mathbb{R}^{m \times l}$  and  $b \in \mathbb{R}^l$ . These linear input constraints can be encoded by the SOS constraints:

$$-a_i p(x) + b_i s(x) \in \mathbf{M}(-B_{\mathcal{I}_t}), \quad (28)$$

where  $a_i$  is the  $i$ th row of  $A$ ,  $i \in \mathcal{I}_t$ , and  $p(x)$  and  $s(x)$  are as in (25). Next, we consider the quadratic input constraint

$$\mathcal{U} = \{u \mid (u - u_0)^T Q_u (u - u_0) \leq u_{\max}^2\}, \quad (29)$$

for some  $Q_u \succeq 0$  and  $u_0 \in \mathbb{R}^m$ . The quadratic input constraint (29) can be encoded using the SOS constraint involving variables  $x \in \mathbb{R}^n$  and  $v \in \mathbb{R}^m$ :

$$-v^T Q_u (p(x) - s(x)u_0) + s(x)u_{\max}^2 \in \mathbf{M}(-f_u, -B_{\mathcal{I}_t}), \quad (30)$$

where  $f_u(x, v) := v^T Q_u v - u_{\max}^2 \in R[x, v]$  encodes the input constraint set in (29). The following lemma establishes the implication of the input constraints based on the SOS constraints. The proof is reported in the appendix.

*Lemma 3:* If  $s(x) > 0$ , a solution  $p(x)$  and  $s(x)$  to the SOS constraint (28), resp. (30), also satisfies the input constraints (27), resp. (29), with  $p(x)/s(x) \in \mathcal{U}$  for all  $x \in \mathcal{X}_s$ .

### C. Safe set and nominal region requirement

In this section, we express the containment conditions of the allowable set  $\mathcal{X}_a$ , the safe set  $\mathcal{X}_s$  and the nominal region  $\mathcal{X}_n$ , as defined in (14) and (10) (cf. Figure 1), in terms of SOS constraints. A slightly more stringent condition compared to (14), can be expressed as the empty-set condition for all  $i \in \mathcal{I}_t$ :

$$\{x \mid B_i(x) \leq 0, w_i(x) \geq 0\} = \emptyset. \quad (31)$$

Using Putinar's P-satz in Theorem 1, we translate (31) into the SOS constraints for all  $i \in \mathcal{I}_t$ :

$$B_i \in \mathbf{M}(w_i). \quad (32)$$

Similarly, the containment condition of  $\mathcal{X}_n$  inside  $\mathcal{X}_s$  in (10), can be expressed as the empty-set condition for all  $i \in \mathcal{I}_t$ :

$$\{x \mid V(x) \leq 0, B_i(x) \geq 0\} = \emptyset. \quad (33)$$

Using Putinar's P-satz, we translate (33) into the SOS constraints for all  $i \in \mathcal{I}_t$ :

$$-B_i \in \mathbf{M}(V). \quad (34)$$

#### D. Resulting SOS problem

The solution to Problem 1, i.e., finding suitable functions  $B_i(x)$ ,  $i \in \mathcal{I}_t$ , and  $V(x)$  can be obtained by solving the following SOS optimization problem:

$$\begin{aligned} &\text{find} && V, B_i, p \in (\mathbb{R}[x])^m, s \in \Sigma[x], \\ &\text{maximize} && \text{vol}(\mathcal{X}_s) \\ &\text{subject to} && (25), (28), (30), (32) \text{ and } (34) \\ &&& s - \epsilon \in \Sigma[x], \end{aligned} \quad (35)$$

where (25) encode the CBF and CLF condition, (28) and (30) encode linear and quadratic input constraints, (32) and (34) encode the set containment properties, and a constant  $\epsilon > 0$  assures that  $s(x) > 0$ .

#### E. Alternating Algorithm

The solution of the SOS problem (35) can be found by iteratively alternate between searching over one set of decision variables while keeping the others fixed, see [8], [11]. In this process, either constraint margins are minimized or the volume of  $\mathcal{X}_s$  is maximized. The volume is approximated by the summation of traces of  $Q_{B_i}$  in  $B_i(x) = Z_{B,i}(x)^T Q_{B,i} Z_{B,i}(x)$ , similar to the approach in [7], [20]. Such an alternating algorithm requires a feasible initialization of the decision variables that are kept fixed in the first iteration. This is achieved through an initialization procedure that starts with an initially empty region of interest and expands it until it encompasses the allowable set  $\mathcal{X}_a$ . For more details, we refer the reader to Section IX.

### V. SAFETY FILTER IMPLEMENTATION

The objective of this section is to implement the advanced safety filter as specified in Problem 2. Given a linear and quadratic input constraints set  $\mathcal{U}$ , we propose the following realization of the Quadratically Constrained Quadratic Program (QCQP) in closed loop for every state  $x \in \mathbb{R}^n$  along the trajectory:

$$\begin{aligned} u_s(x) := & \min_{u \in \mathcal{U}} \|u_n(x) - u\|^2 \\ & \text{s.t.} \quad C(x)u + b(x) \leq r(x), \end{aligned} \quad (36)$$

where

$$C(x) := \begin{bmatrix} \nabla V(x)^T G(x) \\ \nabla B_1(x)^T G(x) \\ \vdots \\ \nabla B_t(x)^T G(x) \end{bmatrix} \quad (37a)$$

$$b(x) := \begin{bmatrix} \nabla V(x)^T f(x) + d(x) \\ \nabla B_1(x)^T f(x) \\ \vdots \\ \nabla B_t(x)^T f(x) \end{bmatrix} \quad (37b)$$

encode the CLF and CBF conditions (15) and (17). The smooth functions  $r(x) = [r_1(x) \ \dots \ r_t(x)]$  are state-dependent slack variables. Within the domain of CLF and CBF conditions (15) and (17), they must satisfy the upper bounds, given by:

$$r_0(x) \leq 0 \quad (38)$$

for all  $x \in \mathcal{X}_t$ , and

$$r_i(x) \leq 0 \quad (39)$$

for all  $i \in \mathcal{I}_t$  and  $x \in \partial\mathcal{X}_s$ . On the one hand, selecting a larger positive value for  $r_0(x)$  within  $\mathcal{X}_n$  (i.e. outside the domain of the CLF condition) increases the allowed dissipation rate violation in terms of larger values of  $\dot{V}(x) = \nabla V(x)^T \dot{x}$ . On the other hand, selecting a larger positive value for  $r_i(x)$ ,  $i \in \mathcal{I}_t$ , within  $\mathcal{X}_s$  (i.e. outside the domain of the CBF condition) increases the allowed safety violation in terms of larger positive values of  $\dot{B}(x) = \nabla B(x)^T \dot{x}$ . This renders the safety filter more passive within the interior of the safe set, and thus leaves more room to satisfy the CLF constraint. However, an overly large value for  $r_i(x)$ ,  $i \in \mathcal{I}_t$ , can result in abrupt modifications of the control action when approaching the boundary of the safe set.

*Remark 4:* In the literature on safety filters, see for example [4], the negative of the allowed dissipation rate and the safety violation are usually specified by class  $\mathcal{K}$  functions  $\alpha(V(x))$  and  $\gamma_i(B_i(x))$ :

$$\nabla V(x)^T (f(x) + G(x)u) \leq -\alpha(V(x)), \quad (40a)$$

$$\nabla B_i(x)^T (f(x) + G(x)u) \leq -\gamma_i(B_i(x)) \quad i \in \mathcal{I}_t. \quad (40b)$$

In this case, the class  $\mathcal{K}$  functions  $\alpha$  and  $\gamma_i$  depend on the value of  $V(x)$  and  $B_i(x)$ . However, in (37), we consider a broader class of the allowed dissipation rate violation  $r_0(x)$  and allowed safety violation,  $r_i(x)$ ,  $i \in \mathcal{I}_t$ , to ensure a smooth safety filter behavior, while satisfying further requirements presented below.

To ensure perfect tracking of the legacy controller  $u_n(x)$  within  $\mathcal{X}_n$  (cf. (9)), we further lower bound  $r(x)$  as:

$$C(x)u_n(x) + b(x) \leq r(x) \quad (41)$$

for all  $x \in \mathcal{X}_n$ . Indeed, condition (41) ensures that the cost of the QCQP in (36) can be minimized to zero within  $\mathcal{X}_n$  with  $u = u_n(x)$ , making  $u_s(x)$  coincide with  $u_n(x) \in \mathcal{U}$ . To ensure existence of  $r(x)$  satisfying lower and upper bounds (38), (39) and (41), we need to show for  $r_0(x)$

that  $\nabla V(x)^T (f(x) + G(x)u_n(x)) + d(x) \leq 0$  on the intersection of  $\mathcal{X}_t$  (cf. (38)) and  $\mathcal{X}_n$  (cf. (41)). This is however directly ensured by forward invariance condition (19). Furthermore, we need to show for  $r_i(x)$ ,  $i \in \mathcal{I}_t$ , that  $\nabla B_i(x)^T (f(x) + G(x)u_n(x)) \leq 0$  on the intersection of  $\partial\mathcal{X}_s$  (cf. (39)) and  $\mathcal{X}_n$  (cf. (41)). This is however automatically satisfied as the domains do not overlap due to the containment condition (10).

Additionally, the selection of  $r(x)$  must be lower-bounded to ensure the feasibility of the QCQP (36) within  $\mathcal{X}_t$ , as (41) already ensures feasibility within  $\mathcal{X}_n$ . Although the exact lower bound is unknown, it can be approximated using a feasible (but not necessarily optimal) solution  $u_{\text{sos}}(x)$  from Section IV:

$$C(x)u_{\text{sos}}(x) + b(x) \leq r(x), \quad (42)$$

for all  $x \in \mathcal{X}_t$ . To guarantee the existence of such an  $r(x)$ , note that the lower bound (42) satisfies the upper bound conditions (38) and (39) as a result of the SOS constraints (25a) and (25b).

Finally, to establish local Lipschitz-continuity of the proposed safety filter, we need the following assumption.

**Assumption 3 (LICQ):** The Linear Independence Constraint Qualification (LICQ) is satisfied for the QCQP in (37) across all states  $x$  and inputs  $u$ , that is, the gradients w.r.t.  $u$  of the active inequality constraints in (37) are linearly independent. Equivalently, the rows of  $C(x)$  associated with the active inequality constraints are linearly independent.

**Remark 5:** By extending the QCQP in (37) with a slack variable  $\delta \in \mathbb{R}^{t+1}$  as in [21]

$$u_s(x) := \underset{\substack{(u,\delta) \in \mathcal{U} \times \mathbb{R}^{t+1} \\ \text{s.t.}}}{\operatorname{argmin}} \quad \|u_n(x) - u\|^2 + \lambda \|\delta\|^2 \\ \text{s.t.} \quad C(x)^T u + b(x) \leq \delta,$$

we automatically satisfy the LICQ property, as demonstrated in [21]. However, the introduction of these slack variables pose the potential risk of compromising safety and finite-time convergence guarantees. That being said, the LICQ assumption can easily be checked, and it generically holds true, i.e., for almost all polynomial coefficients, the Jacobian of a set of polynomials has full rank.

The local Lipschitz-continuity not only preserves existence and uniqueness of solutions (cf. [15][Theorem 3.1]), but can also avoid the resulting feedback controller from chattering, as explained in [22]. The following theorem establishes local Lipschitz-continuity of the developed QCQP controller. Its proof can be found in the appendix.

**Theorem 2:** Under Assumption 3, given a smooth  $B(x)$  and  $V(x)$  as specified in Problem 1, a smooth legacy controller  $u_n(x)$ , and twice differentiable  $r_i(x)$ ,  $i \in \{0\} \cup \mathcal{I}_t$ , lower bounded by (42), then  $u_s(x)$  as defined in (37) is locally Lipschitz-continuous on the safe set  $\mathcal{X}_s$ .

We can find polynomial candidates  $r(x)$  based on given CBF  $B(x)$  and CLF  $V(x)$  by solving an additional SOS problem that encodes the upper and lower bounds (38), (39), (41) and (42).

## VI. POWER CONVERTER CASE STUDY

The proposed safety filter is implemented for a vector field realization of an ac/dc power converter model connected to an

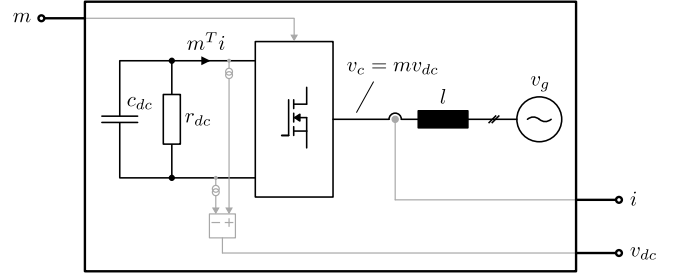


Fig. 5. The schematic is presented in the (dq) rotating frame, comprising a DC-link, 3-phase bridge, and an ac-line connected to an infinite bus  $v_g$ . Assuming the average-value model for the 3-phase bridge, the input  $\bar{u} = [m_d \ m_q]^T$  determines the converter voltage  $v_c$  as a function of the dc-link voltage  $v_{dc}$ . Likewise, the dc-current flowing into the capacitor  $c_{dc}$  is given by the input  $\bar{u}$  and the ac-line current  $i = [i_d \ i_q]^T$ . The states consisting of the dc-link voltage  $v_{dc}$  and the line-current  $i$  are measured.

infinite bus, as illustrated in Figure 5. A feedback controller that avoids unsafe states is crucial for this application since all electrical variables (e.g. voltages and currents) need to be constrained at all times. For more details about the modelling of power converters, we refer the reader to [23].

The signals are represented in the (dq) rotating frame aligned with the phase  $\theta = \omega_n t$  of the grid voltage  $v_g$ , where  $\omega_n = 2\pi 50$  is the nominal angular frequency in Hz. The signals are given in per-unit representation. The system's dynamics are given as follows:

$$(1/\omega_n)c_{dc}\dot{v}_{dc} = -g_{dc}v_{dc} - i_d m_d - i_q m_q \quad (43a)$$

$$(1/\omega_n)\dot{l}i_d = \omega l i_q + v_{dc} m_d - 1 \quad (43b)$$

$$(1/\omega_n)\dot{l}i_q = -\omega l i_d + v_{dc} m_q, \quad (43c)$$

where  $l = 0.01$  is the inductance in p.u. consisting of transformer and line inductance,  $c_{dc} = 0.02$  is the dc-link capacitance in p.u., and  $g_{dc} := 1/r_{dc} = 0.001$  is the admittance of the DC-link capacitor in p.u. The measured states are denoted by  $\bar{x} := [v_{dc} \ i_d \ i_q]^T$ , and the input is given by  $\bar{u} := [m_d \ m_q]^T$ , describing the modulation indices. The objective is to stabilize both the DC-link voltage  $v_{dc}$  to 1, and the quadrature current  $i_q$  to its reference  $i_{q,ref}$ , which is assumed to be constant. As a consequence, to meet the steady-state specifications, the direct current  $i_d$  is stabilized to  $-g_{dc}$ . The allowable set of states must adhere to the following inequality constraints:

$$0.2 \leq v_{dc} \leq 1.2, \quad i_d^2 + i_q^2 \leq (1.2)^2. \quad (44)$$

Furthermore, the quadratic input constraint  $\mathcal{U}$  is given by

$$m_d^2 + m_q^2 \leq (1.2)^2. \quad (45)$$

The system's equilibrium is characterized by

$$x^* = \begin{bmatrix} 1 \\ -g_{dc} \\ i_{q,ref} \end{bmatrix}, u^* = \begin{bmatrix} 1 - \omega l i_{q,ref} \\ -\omega l g_{dc} \end{bmatrix}.$$

We introduce the error coordinates for the states  $x = \bar{x} - x^* = [\tilde{v}_{dc} \ \tilde{i}_d \ \tilde{i}_q]^T$  and the input variables  $u = \bar{u} - u^* = [\tilde{m}_d \ \tilde{m}_q]^T$  such that  $\dot{x} = 0$  at  $x = 0$  and  $u = 0$ . The system



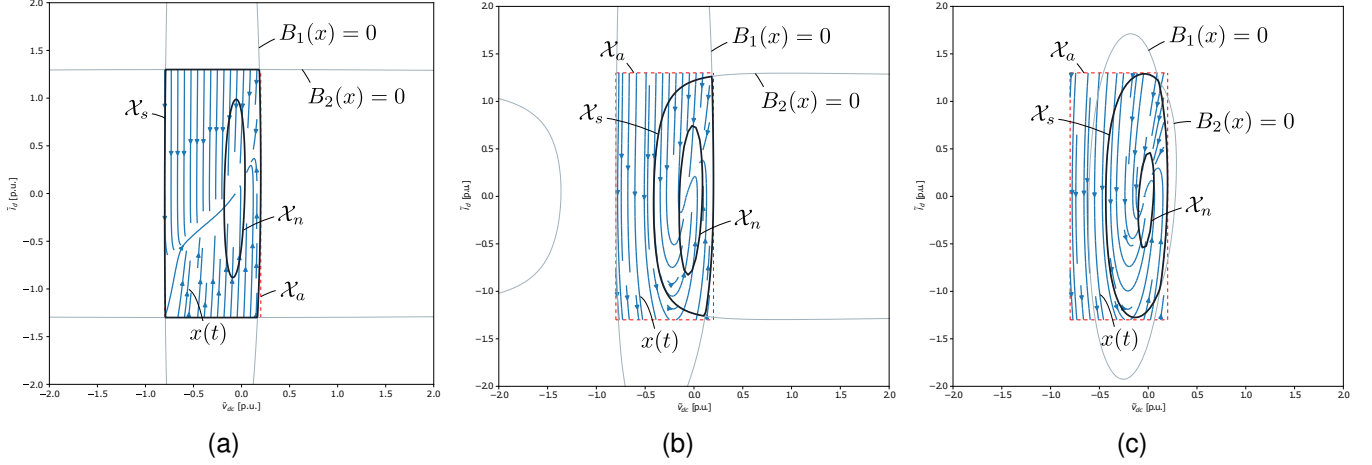


Fig. 6. The allowable set  $\mathcal{X}_a$ , the safe set  $\mathcal{X}_s$ , and the nominal region  $\mathcal{X}_n$  projected to the  $\tilde{v}_{dc}$  and  $\tilde{i}_d$  coordinate are shown for  $\tilde{i}_q = i_{q,ref} = 0$ . In addition, the zero-level sets of the polynomials  $B_1(x)$  and  $B_2(x)$  are shown in grey. Three scenarios are shown, where (a) the input action is subjected to no constraints, i.e.  $u(x(t)) \in \mathbb{R}^m$ , (b) the input action is subjected to a quadratic constraint given by  $u(x(t)) \in \mathcal{U} := \{u \mid u^T u \leq 1.3\}$ , and (c)  $i_{q,ref}$  is integrated as a new state of the dynamical system using the same input constraints. The corresponding vector field  $\dot{x} = f(x) + G(x)u_{sos}(x)$  (projected to  $(\tilde{v}_{dc}, \tilde{i}_d)$  coordinates) is shown in blue, where  $u_{sos}(x) = p(x)/s(x)$  is used to ensure compatibility between the CBF and CLF.

represented in error coordinates is described by system (2) with

$$f(x) = \begin{bmatrix} -0.05\tilde{v}_{dc} - 57.9\tilde{i}_d + 0.00919\tilde{i}_q \\ 1710\tilde{v}_{dc} + 314\tilde{i}_q \\ -0.271\tilde{v}_{dc} - 314\tilde{i}_d \end{bmatrix}$$

$$G(x) = \begin{bmatrix} 0.05 - 57.9\tilde{i}_d & -57.9\tilde{i}_q \\ 1710 + 1710\tilde{v}_{dc} & 0 \\ 0 & 1710 + 1710\tilde{v}_{dc} \end{bmatrix}.$$

We consider a legacy controller that resembles the proportional part of the synchronous rotating frame control structure, as described in [24]:

$$u_n(x) = \begin{bmatrix} 0.1\tilde{v}_{dc} - \tilde{i}_d \\ i_{q,ref} - \tilde{i}_q \end{bmatrix}.$$

In the following subsection, we first consider a single quadrature current reference set to  $i_{q,ref} = 0$ . Then, we introduce a quadrature current reference as a new state to the dynamical system, with a zero time-derivative, i.e.,  $\dot{i}_{q,ref} = 0$ . For each scenario, we find the CBFs  $B_i(x)$  and CLF  $V(x)$  (cf. Problem 1), and perform simulations that illustrate the additional guarantees provided by the advanced safety filter  $u_s(x)$  compared with a standard safety filter implementation. We use CVXOPT Python library to solve the SDPs of the alternating algorithm, and to implement the QCQP in (36). This library implements an optimization problem solver based on second-order and positive semidefinite cones. The simulations are performed using the ODE solver from scipy with a sampling time of 1  $\mu s$ . The full code used for simulations and optimization is publicly available online<sup>1</sup>.

#### A. Zero quadrature current reference tracking

In this subsection, we assume a zero quadrature current reference, i.e.,  $i_{q,ref} = 0$ . The allowable set  $\mathcal{X}_a$ , as expressed

TABLE I  
SUMMARY OF SDP VARIABLES AND CONSTRAINTS

| Scenario  |             | init 1 | init 2 | main 1 | main 2 |
|-----------|-------------|--------|--------|--------|--------|
| Fig. 6(a) | Variables   | 475    | 187    | 410    | 475    |
|           | Constraints | 5726   | 4425   | 5807   | 5726   |
| Fig. 6(b) | Variables   | 506    | 197    | 441    | 506    |
|           | Constraints | 6102   | 4765   | 6183   | 6102   |
| Fig. 6(c) | Variables   | 1086   | 357    | 981    | 1086   |
|           | Constraints | 21277  | 17327  | 21474  | 21277  |

TABLE II  
DEGREE OF THE POLYNOMIALS ENCODING THE CLF, CBF, AND THE RATIONAL CONTROLLER

| $V(x)$ | $B_i(x)$ | $p(x)$ | $s(x)$ |
|--------|----------|--------|--------|
| 4      | 4        | 3      | 2      |

in (12), encoding the state constraints (44), are achieved through the following polynomials:

$$w_1(x) = ((\tilde{v}_{dc} + 0.3)/0.5)^2 + (\tilde{i}_d/20)^2 + (\tilde{i}_q/20)^2 - 1$$

$$w_2(x) = (\tilde{v}_{dc}/20)^2 + (\tilde{i}_d/1.3)^2 + (\tilde{i}_q/1.3)^2 - 1.$$

Figures 6 (a) and (b) illustrates the safe set  $\mathcal{X}_s$  and the nominal set  $\mathcal{X}_n$  computed by the algorithm both without and with considering inputs constraints. Table I summarizes both the number of variables associated with the respective SDPs and the number of constraints, derived from the summation of triangular elements within the positive semidefinite matrices. The initialization procedure completed in 10 iterations, where each iteration took around 10 seconds. The main algorithm completed in 20 iterations, where each iteration took around 14 seconds. The degree of the polynomials are given in Table II.

The proposed safety filter introduces additional guarantees, which make it more stringent and, as noted in the introduction, more suitable in already established industrial setups. However, due these system requirements, it now represents a new category that prioritizes the preservation of the legacy

<sup>1</sup><https://github.com/MichaelSchneeberger/advanced-safety-filter/>

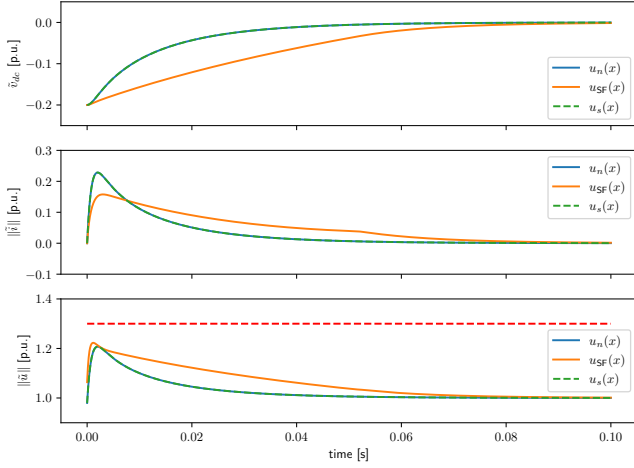


Fig. 7. (Convergence to the nominal region  $\mathcal{X}_n$ ): While the advanced safety filter  $u_s(x)$  essentially overlaps the legacy control  $u_n$ , the basic safety filter  $u_{SF}(x)$  suboptimally perturbs the legacy control action, resulting in a much slower convergence.

control, enhancing composability, preventing a direct performance comparison between conventional safety filters and our novel setup. Nonetheless, side-by-side plots in Figure 7 are included that illustrate the additional guarantees compared to a basic safety filter in selected scenarios. The advanced safety filter  $u_s(x)$  is based on the previously computed CLF  $V(x)$  and CBFs  $B_1(x)$  and  $B_2(x)$ , and is compared to a basic safety filter  $u_{SF}(x)$  using the same CBFs:

$$\begin{aligned} \underset{u \in \mathcal{U}}{\operatorname{argmin}} \quad & \|u_n(x) - u\|^2 \\ \text{s.t.} \quad & \nabla B_1(x)(f(x) + G(x)u) + \alpha(B_1(x)) \leq 0 \\ & \nabla B_2(x)(f(x) + G(x)u) + \alpha(B_2(x)) \leq 0, \end{aligned} \quad (48)$$

where  $\alpha(B_i(x)) := 10B_i(x)$  is selected.

Moreover, a side-by-side plots in Figure 8 illustrate the effect on including quadratic input constraints into the design of the safety filter. We consider the integration of quadratic input constraints into the SOS constraint as a contribution distinct from the discussion on the safety filter's role in preserving the legacy control action. However, for consistency, the simulations were performed using the previous setup, which including an advanced safety filter and the basic safety filter in (48). Since the input constraints are incorporated into the design of the CLF and CBFs, the safety filter  $u_s(x)$  successfully stays within the state constraints for all  $t \geq 0$ . This is not true for a basic safety filter  $u_{SF}(x)$ , which does not consider the input constraints in its design. In this case, the norm of the input action  $\|u_{SF}(x)\|$  exceeds the input constraint limit of 1.3 p.u. in the beginning of the simulation (cf. Figure 8). To produce a valid input, the input action  $u_{SF}(x)$  is projected to the set of feasible input set  $\mathcal{U}$ . As a result, the trajectory deviates from its intended path, leading to a violation of the dc-link voltage constraint.

### B. Including current reference tracking

For this subsection, the objective is to stabilize both the DC-link voltage to 1, and the quadrature current to some (not

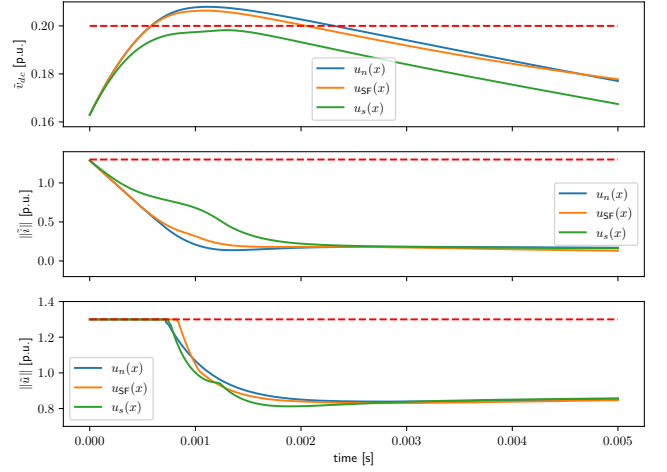


Fig. 8. (Forward invariance of the safe set  $\mathcal{X}_s$ ): While the advanced safety filter  $u_s(x)$ , which considers the quadratic input constraints into the design, successfully stays within the state constraints, whereas the legacy controller  $u_n$  and basic safety filter  $u_{SF}(x)$  violate the state constraints.

yet a priori pre-specified) quadrature current reference  $i_{q,ref}$ . To render our design parametric in  $i_{q,ref}$ , we introduce a new state representing the quadrature current reference. Consequently, we augment the dynamics from (43) with  $\dot{i}_{q,ref} = 0$ .

*Remark 6:* Although the reference  $i_{q,ref}$  is assumed constant for the design of the CBFs and CLF, step-wise adjustments to  $i_{q,ref}$  over time (corresponding to task cycles of the digital processing unit) do not compromise safety, provided the state remains within the safe set  $\mathcal{X}_s$ .

The corresponding coordinates of the states and inputs are given by  $x = [\tilde{v}_{dc} \ \tilde{i}_d \ \tilde{i}_q \ \tilde{i}_{q,ref}]^T$  and  $u := [\tilde{m}_d \ \tilde{m}_q]^T$ , where  $\tilde{i}_{q,ref} = i_{q,ref}$ . The allowable set  $\mathcal{X}_a$  is chosen through the following polynomials:

$$\begin{aligned} w_1(x) &= ((\tilde{v}_{dc} + 0.3)/0.5)^2 + (\tilde{i}_d/20)^2 + (\tilde{i}_q/20)^2 \\ &\quad + (\tilde{i}_{q,ref}/20)^2 - 1 \\ w_2(x) &= (\tilde{v}_{dc}/20)^2 + (\tilde{i}_d/1.3)^2 + (\tilde{i}_q/1.3)^2 \\ &\quad + (\tilde{i}_{q,ref}/20)^2 - 1. \end{aligned}$$

Correspondingly, a safe set  $\mathcal{X}_s$  and the nominal region  $\mathcal{X}_n$  can be computed for this 4-dimensional space. Figure 6(c) illustrates the safe set  $\mathcal{X}_s$  and the nominal set  $\mathcal{X}_n$  for  $i_q = i_{q,ref} = 0$ . Table I summarizes the number of variables of the corresponding SDP for each part, as well as the number of constraints. The initialization procedure completed in 51 iterations, where each iteration took around 60 seconds. The main algorithm completed in 20 iterations, where each iteration took around 90 seconds. The degree of the polynomials are summarized in Table II.

The simulation shown in Figure 9 illustrates the reference tracking performance of our safety filter  $u_s(x)$  compared to the basic safety filter  $u_{SF}(x)$  introduced in the previous subsection. The safety filter, although slightly perturbing the legacy controller, guarantees finite-time convergence to the nominal set defined for a quadrature current reference  $i_{q,ref}$  of 1. However, the basic safety filter  $u_{SF}(x)$  perturbs the legacy control action, leading to a much slower convergence.

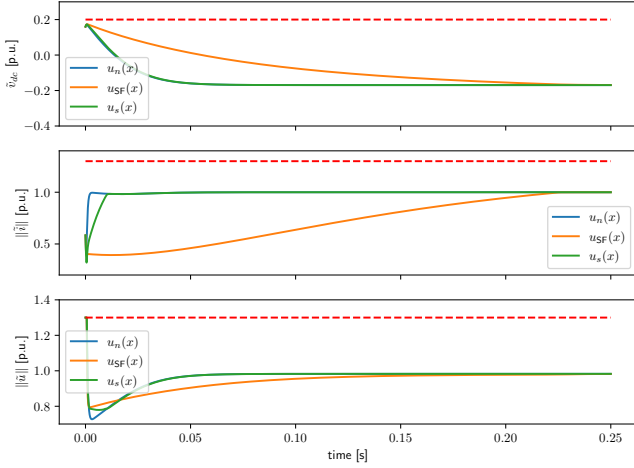


Fig. 9. (Quadrature current reference tracking): The closed-loop simulation demonstrates the finite-time convergence guarantee of the advanced safety filter  $u_s(x)$  towards the nominal region  $\mathcal{X}_n$  for non-zero quadrature current reference  $i_{q,ref} = 1$  p.u. Additionally, the advanced safety filter exhibits a faster convergence to the equilibrium compared to the basic safety filter  $u_{SF}(x)$ . The latter is more likely to disturb the legacy control action as the quadrature current reference  $i_{q,ref}$  approaches the boundary of the safe set, resulting in a slower convergence.

In general, as we approach the boundary of the safe set by increasing  $i_{q,ref}$ , the basic safety filter is more likely to intervene the legacy control action.

## VII. CONCLUSION

We successfully developed and implemented a novel safety filter approach that, to our knowledge, is the first of its kind to leave the existing legacy controller subject to input constraints unaffected. This innovation could lead to greater acceptance of safety filters in industrial environments and real-world scenarios, advancing our understanding of their implementation across a broader range of applications. Our next step is to integrate this safety filter with our industrial partners for the control of an advanced converter topology.

## VIII. APPENDIX

### A. Proof of Lemma 1

Because the safe set  $\mathcal{X}_s$  is compact and forward invariant, and the closed-loop dynamical system  $\dot{x} = f(x) + G(x)u_s(x)$  is Lipschitz-continuous, there exists a unique trajectory  $x(t)$  for all  $x(0) \in \mathcal{X}_s$  and  $t > 0$ . The CLF condition in (17) with  $u := u_s(x)$  can be written without dissipation rate as  $\forall x \in \partial\mathcal{X}_n$ :

$$\nabla V(x)^T (f(x) + G(x)u_s(x)) \leq 0. \quad (49)$$

Using the tangent cone  $T_{\mathcal{X}_n}(x) = \{z \mid \nabla V(x)^T z \leq 0\}$ , the condition (49) can be formulated as  $\forall x \in \partial\mathcal{X}_n$ :

$$f(x) + G(x)u_s(x) \in T_{\mathcal{X}_n}(x).$$

Hence, according to [18, Nagumo's Theorem 4.7],  $\mathcal{X}_n$  is forward invariant. This proves that for all  $x(0) \in \mathcal{X}_n$ , we can choose  $T = 0$ . It remains to show that for all other initial

states, i.e.,  $x(0) \in \mathcal{X}_t$ , there exists  $T \geq 0$  such that  $x(T) \in \mathcal{X}_n$ , or equivalently  $V(x(T)) \leq 0$ .

As  $\mathcal{X}_t \subseteq \mathcal{X}_s$  is compact (cf. Assumption 1) and the dissipative rate  $d(x)$  defined in (18) is assumed to be strictly positive and Lipschitz-continuous on  $\mathcal{X}_t$ , the following minimum exists:  $l = \min_{x \in \mathcal{X}_t} \lambda(x) (V(x) + V_0) > 0$ . Therefore, the scalar function  $V(x(t))$  strictly decreases over time for all  $x(0) \in \mathcal{X}_t$  due to the CLF condition in (17):  $\dot{V} = \nabla V(x)^T (f(x) + G(x)u_s(x)) \leq -l < 0$ . As  $\mathcal{X}_s$  is forward invariant,  $V(x(t))$  is upper bounded by  $V(x(t)) \leq V(x(0)) - lt$  for all  $x(0) \in \mathcal{X}_t$ . Therefore, there exists some  $T \leq V(x(0)) / l$  such that  $V(x(T)) \leq 0$ .

### B. Proof of Lemma 2

By dividing (26a) and (26b) by  $s(x) > 0$ , we obtain

$$\nabla B_i^T (f + Gu_{\text{SOS}}) + \frac{\gamma_{0,i}}{s} B_i - \frac{\gamma_{1,i}^T}{s} B_{\mathcal{I}_t} \leq 0 \quad (50a)$$

$$\nabla V^T (f + Gu_{\text{SOS}}) + d + \frac{\gamma_{0,0}}{s} V - \frac{\gamma_{1,0}^T}{s} B_{\mathcal{I}_t} \leq 0, \quad (50b)$$

where  $u_{\text{SOS}}(x) = p(x)/s(x)$ .

From (50a), by using the fact that  $\gamma_{1,i}(x) \geq 0$ ,  $s(x) > 0$ , and  $B_i(x) = 0$  and  $B_{\mathcal{I}_t}(x) \leq 0$  on  $\partial\mathcal{X}_s$ , we infer, for each  $i \in \mathcal{I}_t$ , that for all  $x \in \partial\mathcal{X}_s$  there exists  $u := u_{\text{SOS}}(x)$  such that  $\nabla B_i^T (f + Gu_{\text{SOS}}) \leq 0$  whenever  $B_i(x) = 0$ . Or, equivalently, for all  $x \in \partial\mathcal{X}_s$  there exists  $u := u_{\text{SOS}}(x)$  such that  $\nabla B_i^T (f + Gu) \leq 0$  for all  $i \in \text{Act}(x)$ , as defined in (16). This proves the CBF condition in (15) using the definition of the tangent cone under Assumption 2.

From (50b), by using the fact that  $\gamma_{0,0}(x) \geq 0$ ,  $\gamma_{1,0}(x) \geq 0$ ,  $s(x) > 0$ , and  $V(x) \geq 0$  and  $B_{\mathcal{I}_t}(x) \leq 0$  on  $\mathcal{X}_t$ , we deduce that for all  $x \in \mathcal{X}_t$  there exists  $u := u_{\text{SOS}}(x)$  such that  $\nabla V^T (f + Gu) + \lambda(V - V_0) \leq 0$ . This proves the CLF condition (17).

Finally, from (26c), by using the fact that  $V(x) = 0$  on  $\partial\mathcal{X}_n$ , we deduce that the inequality  $\nabla V^T (f + Gu_n) \leq 0$  holds for all  $x \in \partial\mathcal{X}_n$ . This proves the CBF condition in (19).

### C. Proof of Lemma 3

We use the definition of a quadratic module in (4), to rewrite the SOS constraint in (28) as  $\forall x \in \mathbb{R}^n, \exists \gamma_u \in (\Sigma[x])^t$ :

$$-a_i u_{\text{SOS}}(x) + b_i + \frac{\gamma_u(x)^T}{s(x)} B_{\mathcal{I}_t}(x) \geq 0$$

for  $i \in \mathcal{I}_t$ , and  $u_{\text{SOS}}(x) = p(x)/s(x)$ . Since the  $\gamma_u(x) \geq 0$ ,  $s(x) > 0$ , and  $B_{\mathcal{I}_t}(x) \leq 0$  on  $\mathcal{X}_s$ , we deduce, for all  $i \in \mathcal{I}_t$ ,  $-a_i u_{\text{SOS}}(x) + b_i \geq 0$  on  $\mathcal{X}_s$ . This concludes the first part of the proof.

By substituting the variable  $v$  in (30) with  $u - u_0$ , we can reformulate the SOS constraints by using the definition of a quadratic module as  $\forall x \in \mathbb{R}^n, \exists \gamma_{u,1} \in \Sigma[x, u], \gamma_{u,2} \in (\Sigma[x, u])^t$ :

$$\begin{aligned} & -((u - u_0)^T Q_u (u_{\text{SOS}}(x) - u_0) - u_{\text{max}}^2) \\ & + \frac{\gamma_{u,1}(x, u)}{s(x)} f_u(x, u - u_0) + \frac{\gamma_{u,2}(x, u)^T}{s(x)} B_{\mathcal{I}_t} \geq 0, \end{aligned} \quad (51)$$

where  $x \in \mathbb{R}^n$  and  $u \in \mathbb{R}^m$  are the variables of the polynomial expressions. Because of its positive semidefiniteness,  $Q_u$  can be decomposed into  $Q_u = B_u^T B_u$ . Furthermore, since  $\gamma_{u,1}(x, u) \geq 0$ ,  $\gamma_{u,2}(x, u) \geq 0$ ,  $s(x) > 0$ ,  $B_{\mathcal{I}_t}(x) \leq 0$  on  $\mathcal{X}_s$ , and  $f_u(x, u - u_0) \leq 0$  on  $\mathcal{U}$ , condition (51) can be reformulated as  $\forall x \in \mathcal{X}_s, \forall u \in \mathcal{U}$ :

$$(u - u_0)^T B_u^T B_u (u_{\text{SOS}}(x) - u_0) \leq u_{\text{max}}^2. \quad (52)$$

For any  $x \in \{x \in \mathcal{X}_s \mid B_u(u_{\text{SOS}}(x) - u_0) = 0\}$ , we have  $(u_{\text{SOS}}(x) - u_0)^T B_u^T B_u (u_{\text{SOS}}(x) - u_0) = 0 \leq u_{\text{max}}^2$ . Hence,  $u_{\text{SOS}}(x) \in \mathcal{U}$ .

For any other safe state, that is  $x \in \{x \in \mathcal{X}_s \mid B_u(u_{\text{SOS}}(x) - u_0) \neq 0\}$ , there exists a unique  $\lambda > 0$  such that

$$(B_u \lambda (u_{\text{SOS}}(x) - u_0))^T (B_u \lambda (u_{\text{SOS}}(x) - u_0)) = u_{\text{max}}^2. \quad (53)$$

Additionally, substituting  $u$  by  $\lambda(u_{\text{SOS}}(x) - u_0) + u_0$  in condition (52) yields the condition that  $\forall x \in \mathcal{X}_s$ :

$$\lambda(B_u(u_{\text{SOS}}(x) - u_0))^T (B_u(u_{\text{SOS}}(x) - u_0)) \leq u_{\text{max}}^2. \quad (54)$$

By comparing (53) and (54), we conclude that  $\lambda$  must be greater than 1. As a consequence,  $(B_u(u_{\text{SOS}}(x) - u_0))^T (B_u(u_{\text{SOS}}(x) - u_0)) \leq u_{\text{max}}^2$  holds for all  $x \in \mathcal{X}_s$ . This concludes that  $u_{\text{SOS}}(x) \in \mathcal{U}$  for all  $x \in \mathcal{X}_s$ .

#### D. Proof of Theorem 2

Consider the optimization problem

$$\begin{aligned} \min_u \quad & f(u, x) \\ \text{s.t.} \quad & g(u, x) \leq 0, \end{aligned} \quad (55)$$

and a point  $x^* \in \mathbb{R}^n$ . We say  $(u_s(x^*), \lambda(x^*))$  is a *regular minimizer* if the LICQ is satisfied at  $u_s(x^*)$ , and  $(u_s(x^*), \lambda(x^*))$  satisfies the KKT condition and the strong second order sufficient condition (SSOSC). The point  $(u, \lambda)$  satisfies the SSOSC if Hessian matrix of the Lagrangian of (55) is positive definite at this point. According to [25, Theorem 2.3.3], there exists a locally Lipschitz continuous map  $u_s(x)$  around a neighborhood of  $x^*$  such that  $u_s(x) \in \mathbb{R}^m$  is a minimizer for the non-linear optimization problem (55), if  $f$  and  $g$  are twice continuously differentiable in  $(u, x)$ , and  $u_s(x^*)$  is a regular minimizer with multiplier  $\lambda(x^*)$ . In what follows, we establish these conditions for the QCQP in (37).

LICQ property under Assumption 3 asserts that for any solution of the QCQP  $u_s(x^*)$ , there exists a unique  $\lambda^*$  that satisfies the KKT condition at  $(u_s(x^*), \lambda^*)$ . Next, we show that the SSOSC holds for any choice of  $\lambda^*$ , specifically  $\lambda^*$  that satisfies the KKT condition. Consider the Lagrangian of the QCQP for either linear or quadratic input constraints:

$$\begin{aligned} L(u, \lambda) = & u^T u + 2u_n(x)u + u_n(x)^T u_n(x) \\ & + \lambda_1^T (C(x)u + b(x)) \\ & + \lambda_2^T (u^T Q_u u - u_{\text{max}}^2) + \lambda_3^T (Au - b) \end{aligned}$$

Then the inequality  $v^T \nabla_{uu}^2 L(u, \lambda) v = v^T v + \lambda_2 v^T Q_u v > 0$  for all  $v \in \mathbb{R}^m$ . This proves that any solution of the QCQP  $u_s(x^*)$  satisfies the SSOSC with the corresponding  $\lambda^*$ . Furthermore, a solution of the QCQP  $u_s(x)$  exists for all  $x$  due to the lower bound on  $r(x)$  in (42), consequently establishing the local Lipschitz continuity of  $u_s(x)$ .

#### REFERENCES

- [1] K.P. Wabersich, A.J. Taylor, J.J. Choi, K. Sreenath, C.J. Tomlin, A.D. Ames, and M.N. Zeilinger. Data-driven safety filters: Hamilton-jacobi reachability, control barrier functions, and predictive methods for uncertain systems. *IEEE Control Systems Magazine*, 43(5):137–177, 2023.
- [2] Athindran Ramesh Kumar, Kai-Chieh Hsu, Peter J Ramadge, and Jaime F Fisac. Fast, smooth, and safe: implicit control barrier functions through reach-avoid differential dynamic programming. *IEEE Control Systems Letters*, 2023.
- [3] M.Z. Romdlony and B. Jayawardhana. Uniting control Lyapunov and control barrier functions. In *53rd IEEE Conference on Decision and Control*, pages 2293–2298. IEEE, 2014.
- [4] A.D. Ames, S. Coogan, M. Egerstedt, G. Notomista, K. Sreenath, and P. Tabuada. Control barrier functions: Theory and applications. In *2019 18th European control conference (ECC)*, pages 3420–3431. IEEE, 2019.
- [5] A.D. Ames, J.W. Grizzle, and P. Tabuada. Control barrier function based quadratic programs with application to adaptive cruise control. In *53rd IEEE Conference on Decision and Control*, pages 6271–6278. IEEE, 2014.
- [6] A. Clark. Verification and synthesis of control barrier functions. In *2021 60th IEEE Conference on Decision and Control (CDC)*, pages 6105–6112. IEEE, 2021.
- [7] L. Wang, D. Han, and M. Egerstedt. Permissive barrier certificates for safe stabilization using sum-of-squares. In *2018 annual American control conference (ACC)*, pages 585–590. IEEE, 2018.
- [8] M. Schneeberger, F. Dörfler, and S. Mastellone. Sos construction of compatible control Lyapunov and barrier functions. *IFAC-PapersOnLine*, 56(2):10428–10434, 2023. 22nd IFAC World Congress.
- [9] H. Wang, K. Margellos, and A. Papachristodoulou. Safety verification and controller synthesis for systems with input constraints. *IFAC-PapersOnLine*, 56(2):1698–1703, 2023.
- [10] H. Dai and F. Permenter. Convex synthesis and verification of control-Lyapunov and barrier functions with input constraints. In *2023 American Control Conference (ACC)*, pages 4116–4123. IEEE, 2023.
- [11] W. Tan and A. Packard. Searching for control Lyapunov functions using sums of squares programming. *sibi*, 1(1), 2004.
- [12] P. Zhao, R. Ghabcheloo, Y. Cheng, H. Abdi, and N. Hovakimyan. Convex synthesis of control barrier functions under input constraints. *IEEE Control Systems Letters*, 2023.
- [13] A. Isaly, M. Ghanbarpour, R.G. Sanfelice, and W.E. Dixon. On the feasibility and continuity of feedback controllers defined by multiple control barrier functions for constrained differential inclusions. In *2022 American Control Conference (ACC)*, pages 5160–5165. IEEE, 2022.
- [14] G. Valmorbidia and J. Anderson. Region of attraction estimation using invariant sets and rational Lyapunov functions. *Automatica*, 75:37–45, 2017.
- [15] H.K. Khalil. *Nonlinear Systems*. Pearson Education. Prentice Hall, 2002.
- [16] P. Wieland and F. Allgöwer. Constructive safety using control barrier functions. *IFAC Proceedings Volumes*, 40(12):462–467, 2007.
- [17] M. Laurent. Sums of squares, moment matrices and optimization over polynomials. *Emerging applications of algebraic geometry*, pages 157–270, 2009.
- [18] F. Blanchini. Set invariance in control. *Automatica*, 35(11):1747–1767, 1999.
- [19] Michael Schneeberger, Silvia Mastellone, and Florian Dörfler. Advanced safety filter based on sos control barrier and lyapunov functions. *arXiv preprint arXiv:2401.06901*, 2024.
- [20] S. Kundu, S. Geng, S.P. Nandanoori, I. A. Hiskens, and K. Kalsi. Distributed barrier certificates for safe operation of inverter-based microgrids. pages 1042–1047, 2019.
- [21] A.D. Ames, X. Xu, J. W. Grizzle, and P. Tabuada. Control barrier function based quadratic programs for safety critical systems. *IEEE Transactions on Automatic Control*, 62(8):3861–3876, 2016.
- [22] B. Morris, M.J. Powell, and A.D. Ames. Sufficient conditions for the lipschitz continuity of qp-based multi-objective control of humanoid robots. In *52nd IEEE Conference on Decision and Control*, pages 2920–2926. IEEE, 2013.
- [23] N. Mohan, T. M. Undeland, and W.P. Robbins. *Power electronics: converters, applications, and design*. John wiley & sons, 2003.
- [24] F. Blaabjerg, R. Teodorescu, M. Liserre, and A.V. Timbus. Overview of control and grid synchronization for distributed power generation systems. *IEEE Transactions on industrial electronics*, 53(5):1398–1409, 2006.
- [25] K. Jittorntrum. *Sequential algorithms in nonlinear programming*. The Australian National University (Australia), 1978.

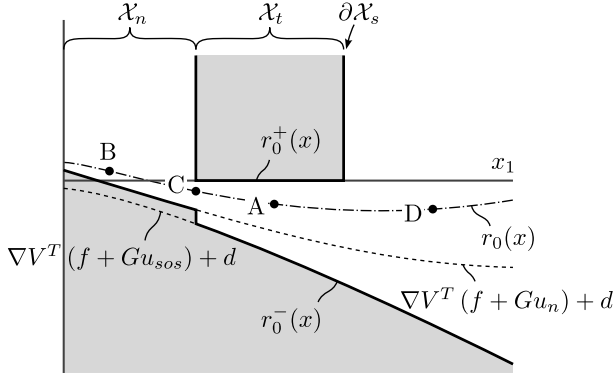


Fig. 10. (Upper and lower bounds on  $r_0(x)$ ): Whereas the upper bound  $r_0^+(x)$  is directly given by the CLF condition in (17), only an estimate of the lower bound  $r_0^-(x)$  can be obtained by the solution of the SOS constraints in (35) involving  $u_{\text{sos}} := p(x)/s(x)$  and the legacy controller  $u_n(x)$ .

## IX. SUPPLEMENTARY MATERIAL

### A. Derivation of the SOS constraints (24)

The objective of this section is to convert the empty-set condition (23b) into the SOS constraint given in (24b). The derivation of (24a) and (24c) is analogous. Applying Putinar's P-satz to (23b) yields the SOS constraint

$$-\nabla V^T f - d \in \mathbf{M}(\nabla V^T G, -\nabla V^T G, V, -B_{\mathcal{I}_t}).$$

By utilizing the definition of a quadratic module in (4), we can express this SOS constraint by the condition that there exist two SOS polynomials  $p_{0,1}, p_{0,2} \in (\Sigma[x])^m$  such that

$$-\nabla V^T (f + G(p_{0,1} - p_{0,2})) - d \in \mathbf{M}(V, -B_{\mathcal{I}_t}).$$

By exploiting the fact that the set of SOS polynomials, when combined with the set of negative SOS polynomials, spans the entire set of polynomials (i.e.,  $\Sigma[x] - \Sigma[x] = R[x]$ ), we can reformulate the SOS constraint as the condition that there exists a polynomial  $p_0 \in (R[x])^m$  such that

$$-\nabla V^T (f + Gp_0) - d \in \mathbf{M}(V, -B_{\mathcal{I}_t}).$$

Finally, we introduce an additional SOS polynomial  $s_0(x)$  (cf. (7)) and rewrite the SOS constraint as the condition that there exists  $s_0 \in \Sigma[x]$ ,  $p_0 \in (R[x])^m$  such that

$$-\nabla V^T (s_0 f + Gp_0) - s_0 d \in \mathbf{M}(V, -B_{\mathcal{I}_t}).$$

The introduction of the polynomial  $s_0(x)$  increases the set of feasible solutions when truncating the degrees of the involved polynomials, as described in Section II-B.

### B. Lower and upper bounds of $r_0(x)$

We illustrate a typical design choice for  $r_0(x)$ , as defined in (36), in Figure 10.

For states inside the transitional region  $x \in \mathcal{X}_t$  (see point A in Figure 10),  $r_0(x)$  is required to be smaller than the upper bound  $r_0^+(x) = 0$  for (37) to satisfy the CLF condition in (17). On the other hand, an estimate of the lower bound on  $r_0(x)$  can be obtained from the solution  $u_{\text{sos}}(x) = p(x)/s(x)$  of the SOS problem in (35). The corresponding lower bound is then given by  $r_0^-(x) = \nabla V(x)^T (f(x) + G(x)u_{\text{sos}}(x)) + d(x)$ ,

which is smaller than the upper bound  $r_0^+(x) = 0$  within  $\mathcal{X}_t$  due to (26b). We wish to emphasize that there may exist more optimal lower bounds on  $r_0(x)$ ; however, the one chosen is certified by the SOS constraints developed in the previous chapter.

For states inside the nominal region  $x \in \mathcal{X}_n$  (see point B in Figure 10), no upper bound is specified. Hence, by selecting a large  $r_0(x)$ , we can relax the corresponding constraint of the QCQP in (37). Applying the same approach to other  $r_i(x)$  allows us to enlarge the feasible set until  $u := u_n(x)$  is a feasible solution for the QCQP, required to satisfy (9). Therefore, we propose the following lower bound:  $r_0^-(x) = \nabla V(x)^T (f(x) + G(x)u_n(x)) + d(x)$ . By assigning  $u := u_n(x)$ , the corresponding constraint of the QCQP, expressed as  $r_0^-(x) - r_0(x) \leq 0$ , is clearly satisfied.

For states on the boundary of the nominal region  $x \in \partial\mathcal{X}_n$  (see point C in Figure 10), we must ensure compatibility of the lower and upper bounds discussed in the previous paragraphs. More concretely, we need to ensure that  $\nabla V(x)^T (f(x) + G(x)u_n(x)) + d(x) \leq 0$  for all  $x \in \partial\mathcal{X}_n$ . However, this inequality follows directly from inequality (26c).

Finally, for states outside the safe set  $x \notin \mathcal{X}_s$  (see point D in Figure 10), an upper bound on  $r(x)$  is not specified. The lower bound can be chosen as in A. It is however important to note that the region can be made attracting with respect to the safe set by the additional requirement of selecting a negative  $r(x)$ . This can restore the system state to the safe set in scenarios where unexpected system noise or model mismatch cause the system to deviate from the safe set.

### C. Alternating Algorithm

The solution of the SOS problem (35) presents a particular challenge due to its bilinearity, i.e., the simultaneous search for CBF  $B(x)$ , CLF  $V(x)$ , a rational controller  $u_{\text{sos}}(x)$ , and other SOS polynomials introduced by the Positivstellensatz. This bilinearity prevents us from converting the SOS problem directly into a Semi-Definite Program (SDP). Similar to [8], [11], however, we can iteratively alternate between searching over one set of decision variables while keeping the others fixed. Such an alternating algorithm requires a feasible initialization of the decision variables that are kept fixed in the SDP of the first iteration. Therefore, we propose an initialization procedure to find such an initial set of feasible parameters following the presentation of the main algorithm.

### D. Main algorithm

To make the main algorithm compatible with the initialization procedure, we introduce an *operating region* that contains the allowable set  $\mathcal{X}_a$ :

$$\mathcal{X}_{\text{op}} := \{x \mid f_{\text{op}}(x) \leq 0\} \supseteq \mathcal{X}_a, \quad (56)$$

with scalar polynomial  $f_{\text{op}} \in R[x]$ . We assume that there exists a constant  $\rho_{\Sigma} \in \mathbb{R}$  such that

$$f_{\text{op}}(x) + \rho_{\Sigma} \in \Sigma[x] \quad (57)$$

is an SOS polynomial. This assumption, while not overly restrictive, is important for establishing the feasibility of the

SDP in *Part 1* of the initialization procedure, as elaborated in the subsequent subsection.

*Remark 7:* The operating region  $\mathcal{X}_{op}$  can be determined by solving another SOS problem, as condition (57) directly translates to an SOS constraint. By making minor adjustments, it is possible to define the operating region  $\mathcal{X}_{op}$  using multiple polynomials, and it could even coincide with the allowable set  $\mathcal{X}_a$ . However, in order to reduce computational complexity, we restrict the number of polynomials to one. In cases, where the operating region  $\mathcal{X}_{op}$  closely approximates the safe set  $\mathcal{X}_s$ , the polynomials  $B_i(x)$  in the quadratic modules of the SOS problem in (35) can be omitted, thereby reducing the total number of decision variables. This will reduce computational complexity by introducing slightly more conservative SOS constraints.

The constraint  $f_{op}(x) \leq 0$  defining the operating region  $\mathcal{X}_{op}$  is added to the empty set conditions (23) developed in Section IV. From a set-theoretic point of view, adding the constraint  $f_{op}(x) \leq 0$  does not alter the empty set conditions, given that  $\mathcal{X}_s \subseteq \mathcal{X}_{op}$ . However, by applying Putinar's P-satz on the empty set conditions (23) including  $f_{op}(x) \leq 0$ , we obtain slightly different SOS constraints for all  $i \in \mathcal{I}_t$ :

$$-\nabla V^T(sf + Gp) - sd \in \mathbf{M}(V, -B_{\mathcal{I}_t}, -f_{op}) \quad (58a)$$

$$-\nabla B_i^T(sf + Gp) \in \mathbf{M}(B_i, -B_{\mathcal{I}_t}, -f_{op}) \quad (58b)$$

$$-\nabla V^T(f + Gu_n) - d \in \mathbf{M}(V, -V, -f_{op}). \quad (58c)$$

These SOS constraints are used to define the main algorithm.

The main algorithm involves alternating between two SDPs, as described by *Part 1* and *Part 2* below. Given an initial set of feasible parameters, the SDP in *Part 1* is guaranteed to be feasible for each iteration when utilizing the solution from *Part 2*. Likewise, the SDP in *Part 2* is guaranteed to be feasible for each iteration when utilizing the solution from *Part 1*. Furthermore, as shown in [8], the cost of the SDP in *Part 1* encoding the volume of the safe set is non-decreasing over the iterations.

*Part 1 - Searching for CBF and CLF:* In the first part, we search over CBFs  $B_i(x)$  and a CLF  $V(x)$  that maximize the volume of the safe set. To make the SDP computationally tractable, we approximate the volume of the safe set by the summation of traces of  $Q_{B_i}$ , similar to [7], [20]:

$$\begin{aligned} &\text{find} && V, B_i \in R[x] \\ &\text{hold fixed} && p, s \\ &\text{maximize} && \sum_{i \in \mathcal{I}_t} \text{tr}(Q_{B_i}) \\ &\text{subject to} && (32), (34) \text{ and } (58), \end{aligned}$$

where the  $Q_{B_i}$  are derived from the decomposition of the CBF  $B_i(x)$  into  $B_i(x) = Z_{B,i}(x)^T Q_{B,i} Z_{B,i}(x)$  (cf. (1)).

*Part 2 - Searching for a controller:* For the second part of the main algorithm, we search over a rational controller  $u_{\text{SOS}}(x) = p(x)/s(x)$  that maximizes the SOS constraint margins, denoted by  $\Delta_i \in \mathbb{R}$ ,  $i \in \{0\} \cup \mathcal{I}_t$ . Only the first two SOS constraints from (58) depend on the rational controller. They are specified with the inclusion of these margins  $\Delta_i$  as:

$$-\nabla V^T(sf + Gp) - sd + \Delta_0 \in \mathbf{M}(B_i, -B_{\mathcal{I}_t}, -f_{op}) \quad (59a)$$

$$-\nabla B_i^T(sf + Gp) + \Delta_i \in \mathbf{M}(B_i, -B_{\mathcal{I}_t}, -f_{op}) \quad (59b)$$

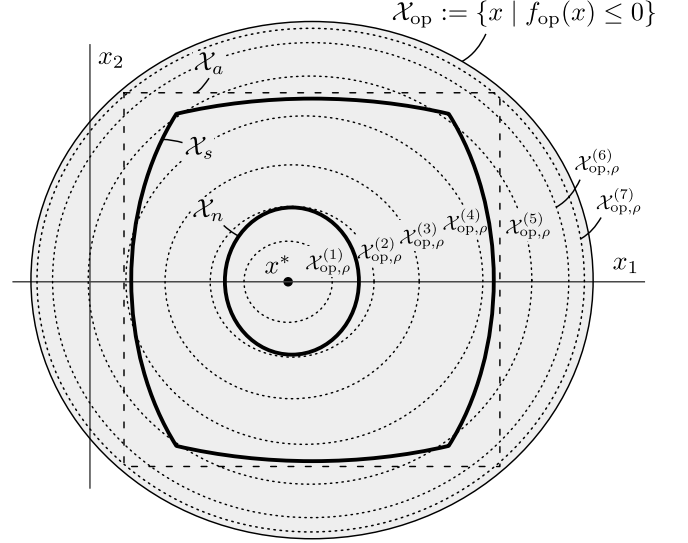


Fig. 11. (Operating region): The initialization procedure produces an initial set of feasible parameters for the main algorithm by iteratively expanding the operating region  $\mathcal{X}_{op,\rho}$ . The initialization procedure finishes if  $\mathcal{X}_{op} = \mathcal{X}_{op,\rho}^{(k)}$ .

for all  $i \in \mathcal{I}_t$ . Large values of  $\Delta_i$ ,  $i \in \{0\} \cup \mathcal{I}_t$ , will increase the set of feasible solution in *Part 1* in the subsequent iterations. The SDP involved in *Part 2* is given by:

$$\begin{aligned} &\text{find} && p \in (\mathbb{R}[x])^m, s \in \Sigma[x], \Delta_i \in \mathbb{R} \\ &\text{hold fixed} && V, B_i \\ &\text{maximize} && \sum_{i \in \{0\} \cup \mathcal{I}_t} \Delta_i \\ &\text{subject to} && (28), (29) \text{ and } (59) \\ &&& s - \epsilon \in \Sigma[x], \Delta_{\min} \leq \Delta_i. \end{aligned} \quad (60)$$

A constant  $\epsilon > 0$  assures that  $s(x) > 0$ . The minimum margin  $\Delta_{\min} < 0$  is selected to maintain numerical stability of the algorithm. The main algorithm concludes when the increment in  $\sum_{i \in \mathcal{I}_t} \text{tr}(Q_{B_i})$  in *Part 1* does not exceed a predefined minimal threshold.

### E. Initialization procedure

The main algorithm, presented in previous subsection, requires an initial set of feasible parameters. Therefore, we present an initialization procedure to find such an initial set.

Similar to the main algorithm, the initialization procedure involves an alternating between two SDPs, as described by *Part 1* and *Part 2* below. The feasibility of each part is guaranteed by employing the solution of the SDP from the previous iteration. To make sure that the SDP in *Part 1* is feasible in the first iteration, we use a modified operating region (cf. (56))

$$\mathcal{X}_{op,\rho} := \{x \mid f_{op}(x) + \rho \leq 0\}, \quad (61)$$

with  $\rho \geq 0$ . By choosing the  $\mathcal{X}_{op,\rho}$  initially sufficiently small in volume, i.e., a large  $\rho > 0$ , we guarantee feasibility of the SDP in *Part 1* for any initial set of parameters, as shown in Lemma 4.



By applying Putinar's P-satz on the modified empty set condition (23) including  $f_{\text{op}} + \rho \leq 0$  instead, we derive the following SOS constraints for all  $i \in \mathcal{I}_t$ :

$$-\nabla V^T (sf + Gp) - sd \in \mathbf{M}(V, -B_{\mathcal{I}_t}, f_{\text{op}} + \rho) \quad (62a)$$

$$-\nabla B_i^T (sf + Gp) \in \mathbf{M}(B_i, -B_{\mathcal{I}_t}, f_{\text{op}} + \rho) \quad (62b)$$

$$-\nabla V^T (f + Gu_n) - d \in \mathbf{M}(V, -V, f_{\text{op}} + \rho). \quad (62c)$$

*Part 1 - Searching for CBF and CLF:* The first part of the initialization procedure searches over CBF and a CLF that maximize  $\rho$ , thereby increasing the volume of  $\mathcal{X}_{\text{op}, \rho}$  for every iteration (cf. Figure 11). To make sure that  $\mathcal{X}_{\text{op}, \rho}$  is contained in the operating region, i.e.,  $\mathcal{X}_{\rho}^{(k)} \subseteq \mathcal{X}_{\text{op}}$ , we impose the constraint that  $0 \leq \rho$ . The resulting SDP is expressed as:

$$\begin{aligned} &\text{find} && V, B_i \in R[x], \rho \in \mathbb{R} \\ &\text{hold fixed} && p, s \\ &\text{maximize} && \rho \geq 0 \\ &\text{subject to} && (32), (34) \text{ and } (62). \end{aligned} \quad (63)$$

The next lemma establishes feasibility of the SDP (63) in the first iteration. Its proof can be found in the appendix.

*Lemma 4:* Assuming that there exist candidates  $V(x)$  and  $B_i(x)$  that satisfy conditions (32) and (34), then the SDP in (63) is feasible using random initial coefficient values for polynomials  $p(x) \in (R[x])^m$  and  $s(x) \in \Sigma[x]$ .

*Proof:* By utilizing the definition of a quadratic module in (4), the conditions in (62) can be formulated as the existence of  $\gamma_{0,i}, \gamma_n \in R[x]$ ,  $\gamma_{0,0}, \gamma_{\text{op},0}, \gamma_{\text{op},i}, \gamma_{\text{op},n} \in \Sigma[x]$ , and  $\gamma_{1,i}, \gamma_{1,0} \in (\Sigma[x])^t$  such that

$$q_i + \gamma_{\text{op},i}(f_{\text{op}} + \rho) \in \Sigma[x] \quad (64a)$$

$$q_0 + \gamma_{\text{op},0}(f_{\text{op}} + \rho) \in \Sigma[x] \quad (64b)$$

$$q_n + \gamma_{\text{op},n}(f_{\text{op}} + \rho) \in \Sigma[x], \quad (64c)$$

with polynomials

- $q_i := -\nabla B_i^T (sf + Gp) - \gamma_{0,i}B_i + \gamma_{1,i}^T B_{\mathcal{I}_t}$
- $q_0 := -\nabla V^T (sf + Gp) - sd - \gamma_{0,0}V + \gamma_{1,0}^T B_{\mathcal{I}_t}$
- $q_n := -\nabla V^T (f + Gu_n) - d + \gamma_n V$ .

First, we show that for any polynomial  $q \in R[x]$ , we can find  $\gamma_{\text{op}} \in \Sigma[x]$  and  $\rho \in \mathbb{R}$  such that

$$q(x) + \gamma_{\text{op}}(x)(f_{\text{op}}(x) + \rho) \in \Sigma[x]. \quad (65)$$

To show this, we select an SOS polynomial  $\gamma_{\text{op}} \in \Sigma[x]$  sufficiently large such that  $q(x) + \gamma_{\text{op}}(x) \in \Sigma[x]$ . This is always possible since starting from the decomposition  $q(x) = Z(x)^T Q_f Z(x)$  (cf. (1)), we can select  $\gamma_{\text{op}}(x) = \nu Z(x)^T Z(x)$ , with arbitrary large  $\nu > 0$ , such that  $Q_f + \nu I \succ 0$ . Second, by utilizing the assumption on  $\rho_{\Sigma}$  (cf. (57)), choose  $\rho := \rho_{\Sigma} + 1$  such that  $q(x) + \gamma_{\text{op}}(x) + \gamma_{\text{op}}(x)(\rho(x) + \rho_{\Sigma}) \in \Sigma[x]$ . Hence, any  $\rho \geq \rho_{\Sigma} + 1$  renders (65) an SOS polynomial.

In this way, we can find  $\rho$  for each SOS constraint in (64), and denote them by  $\rho_0, \rho_i, \rho_n \in \mathbb{R}$ . By selecting  $\rho := \max(\rho_0, \rho_i, \rho_n)$ , all SOS constraints in (64) hold simultaneously. Hence, the SOS problem (63) is feasible for any initialization of  $q_0(x)$ ,  $q_i(x)$ ,  $i \in \mathcal{I}_t$ , and  $q_n(x)$ . ■

*Part 2 - Searching for a controller:* Similar to the main algorithm, we search over a rational controller  $u_{\text{SOS}}(x) = p(x)/s(x)$  that maximizes the SOS constraint margins, denoted by  $\Delta_i \in \mathbb{R}$ ,  $i \in \{0\} \cup \mathcal{I}_t$ . The corresponding SOS constraints including these margins  $\Delta_i$  are specified as:

$$-\nabla V^T (sf + Gp) - d + \Delta_0 \in \mathbf{M}(V, -B_{\mathcal{I}_t}, f_{\text{op}} + \rho) \quad (66a)$$

$$-\nabla B_i^T (sf + Gp) + \Delta_i \in \mathbf{M}(B_i, -B_{\mathcal{I}_t}, f_{\text{op}} + \rho), \quad (66b)$$

for all  $i \in \mathcal{I}_t$ . The resulting SDP is given by:

$$\begin{aligned} &\text{find} && p \in (\mathbb{R}[x])^m, s \in \Sigma[x], \Delta_i \in \mathbb{R} \\ &\text{hold fixed} && V, B_i, \rho \\ &\text{maximize} && \sum_{i \in \{0\} \cup \mathcal{I}_t} \Delta_i \\ &\text{subject to} && (28), (29) \text{ and } (66), \\ &&& s - \epsilon \in \Sigma[x], \Delta_{\min} \leq \Delta_i. \end{aligned}$$

A constant  $\epsilon > 0$  assures that  $s(x) > 0$ . Similar to the SDP (60), the minimum margin  $\Delta_{\min} < 0$  is selected to maintain numerical stability of the algorithm. The initialization procedure is considered complete when  $\rho = 0$ , i.e.,  $\mathcal{X}_{\rho}^{(k)} = \mathcal{X}_{\text{op}}$ . At this point, we found an initial set of feasible parameters for the SDP in *Part 1* of the main algorithm.

*Remark 8:* The initialization procedure can be extended with additional steps where the margins  $\Delta_i$  are introduced when searching over the controller, or the operational region is expanded – by decreasing  $\rho$  – when searching for CBF and CLF. Furthermore, we can introduce additional steps where we optimize only over a subset of the  $\Delta_i$ 's.